# ABSTRACT

AGRAWAL, MANISHA. Formation of β-Cyclodextrin Inclusion Complex with a Phenolic Antioxidant and its Industrial application in Polyethylene Film. (Under the guidance of Dr. Hyun Suk Whang)

Butylated hydroxytoluene (BHT) is a phenolic antioxidant, which is primarily used in food additives. Due to its high volatility, it can be suspected to have losses through volatilization in high temperature applications. However, there is barely any research work focused on the formation of BHT-β-CD-IC. In this study, we have successfully formed the inclusion compound between BHT and β-CD (BHT-β-CD-IC) and characterized it using wide-angle x-ray diffraction (WAXD), differential scanning calorimetry (DSC), thermogravimetric analysis (TGA), nuclear magnetic resonance spectroscopy (NMR) and ultra violet visible spectroscopy (UV-Vis).

We produced on pilot scale three sets of low density polyethylene (LDPE) films with the addition of BHT, β-CD, and BHT-β-CD-IC. The determination of BHT content in the films was carried out using Gas Chromatography- Mass Spectrometry (GC-MS). The results show that 44% BHT was lost from BHT-β-CD-IC LDPE films while 78% BHT was lost from the BHT LDPE film. Hence, the complex proved to be more efficient in preventing loss of BHT due to encapsulation of volatile guest. In addition, microscopy studies indicate that BHT-β-CD-IC LDPE film shows small aggregates uniformly distributed over a large range in the LDPE matrix.

The oxidative performance of the films was studied using differential scanning calorimetry (DSC) for determining the oxidation induction time ($OIT_{time}$) and oxidation induction temperature ($OIT_{temp.}$). It was found that $OIT_{temp.}$method is less sensitive as compared to the $OIT_{time}$ method. The $OIT_{time}$ was 35 min for the BHT-β-CD-IC

LDPE film as compared with 16 min and 26 min values of LDPE and BHT LDPE films, respectively. Hence, the encapsulation of BHT in the CD maximizes the efficiency and stability to thermal degradation for BHT-β-CD-IC film. The viscoelastic behavior of the films was also studied using dynamic mechanical analysis (DMA). The results indicate increases in storage modulus ($E^{I}$) and loss modulus of the complex ($E^{II}$) and a shift in the maxima of tan $\delta$ ($E^{II}/E^{I}$) to lower temperature in the LDPE films processed with BHT, β-CD and BHT-β-CD-IC.

# Synthesis of β-Cyclodextrin Inclusion Complex with Phenolic Antioxidant in Polyethylene Film and its Industrial Applications

by
Manisha Agrawal

A thesis submitted to the Graduate Faculty of
North Carolina State University
In partial fulfillment of the
Requirements for the degree of
Master of Science

Textile Chemistry

Raleigh, North Carolina

June 2008

APPROVED BY:

| | |
|---|---|
| Samuel M. Hudson | C.M. Balik |
| Hyun Suk Whang, Co-Chair | Alan E. Tonelli, Co-Chair |

## DEDICATION

# TO MY PARENTS

# BIOGRAPHY

Manisha Agrawal is currently a Master's student at Department of Textile Engineering, Chemistry & Science, College of Textiles, North Carolina State University, NC, USA. She received her Bachelor's degree in Textile Technology from Rajiv Gandhi Technical University, S.V.I.T.S., Indore, India. She is currently working on the synthesis and characterization of cyclodextrin inclusion complexes with active component in polymer films and their industrial applications.

# ACKNOWLEDGEMENTS

I would like to express my most sincere appreciation to my co-advisor, Dr. Hyun Suk Whang, for her advice, guidance, support, encouragement and many hours of helpful discussions which made this research possible. I would also like to thank other committee members for their support, Dr. Alan E. Tonelli who is my co-chair, Dr. Sameul M. Hudson, committee member and Dr. C. Maurice Balik, who is my minor representative from the Department of Materials Science and Engineering.

I would like to thank Birgit Anderson (Analytical Lab Manager) for giving me the analytical instrumentation training, Judy Elson for providing help in microscopy experiments, Plastics Color Corporation and Clemson Packaging Center for compounding and extruding polymer films on pilot scale, Dr. Laxminath Sripada for Nuclear Magnetic Resonance Spectroscopy data analysis, United States Department of Agriculture (USDA) for GC-MS equipment and data analysis and Mrs. Penny Amato for oxidation induction time and temperature studies via DSC. Finally I would like to thank Kapil Agrawal, Sandeep Navada and Sridevi Seshabhattar for their help and support.

# TABLE OF CONTENTS

# LIST OF FIGURES

# LIST OF TABLES

# I. LITERATURE REVIEW

## 1. CYCLODEXTRINS

### 1.1 Historical Background

The development of cyclodextrin (CDs) chemistry consists of three periods. During the first period (1891-1935), CDs were originally termed by Villiers in 1891 [1] as “cellulosine” due to their similarity to cellulose in being relatively resistant to hydrolysis. Until 1935, CDs were discovered without elucidating exact chemical structures and recognizing their practical potential. In the second period (1936-1970), by the end of 1960s, their structures, physical, and chemical properties as well as the inclusion complex forming properties of their cavities had been discovered [2]. In addition, methods for the laboratory scale preparation of CDs were established. In the third period, (1970 to present), the research is aimed at the industrial production and utilization of CDs, and is called the, “applied research” period [3].

### 1.2 Structures

Cyclodextrins are oligosaccharides produced by glucosyltransferase enzymatic degradation of amylase starch. CDs are composed of $\alpha$-(1,4)-linked D(+)-glucopyranose units and make up a family of three well-known cyclic members; $\alpha$-, $\beta$-, and $\gamma$-CDs containing six, seven, and eight monosaccharide moieties, respectively. As a result of the C-1 (chair) conformation of each D-glucose residue

and the lack of free rotation about the glycosidic bonds, which connect the glucose units, CDs have the shape of a hollow truncated cone as shown in Figure 1. All hydroxyl groups are directed towards the exterior of the cyclodextrin cone. The secondary hydroxyl groups (on the C-2 and C-3 atoms of glucose units) are located on one side of the torus. They are more open than the primary hydroxyl groups (on the C-6 atoms of glucose units) which are located on the opposite side of the torus. On the other hand, two rings of the non-exchangeable hydrogen atoms (H-3 and H-5) and the glycosidic oxygens are located on the interior of the cavity. Hence, the interior of the torus is relatively hydrophobic compared with the hydrophilic external surface as shown in Figure 1. Table 1 lists some molecular and dimensional parameters of cyclodextrins [4, 5, 6, 7].

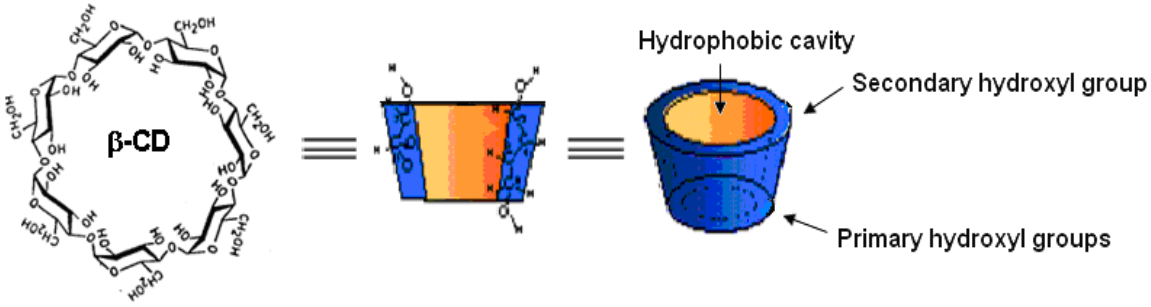


**Figure1**. Cyclodextrin structures

**Table 1.** Important molecular parameters of α-, β- and γ-cyclodextrins

| **Parameters** | **α-CD** | **β-CD** | **γ-CD** |
|---|---|---|---|
| Glucose residues | 6 | 7 | 8 |
| Molecular weight | 973 | 1135 | 1297 |
| Cavity diameter (A°) | 4.7-5.3 | 6-6.6 | 7.5-8.3 |
| Cavity height (A°) | 7.9 | 7.9 | 7.9 |
| Cavity volume ($A^{\circ 3}$) | 174 | 262 | 472 |

## 1.3 Chemical and Physical Properties

CDs are stable in alkaline solution even at elevated temperatures. CDs are more resistant to acid hydrolysis than starch, although strong acids such as sulfuric or hydrochloric acid can hydrolyze CDs. Upon acid hydrolysis they release glucose as by product. The rate of acid hydrolysis increases as a function of increased acid concentration, type of acid, and temperature. Thermal analysis shows that the thermal decomposition of CDs occurs at about 300$^{o}$C. Hence, CDs are thermally stable. Solubility in water differs significantly among the three CDs, although the solubility of all three CDs increase as temperature is increased. The water solubility of $\alpha$, $\beta$ and $\gamma$-CD is 14.5, 1.85, and 23.2 g/100 mL at 25$^{o}$C. The solubility of $\beta$-CD is much lower than those of $\alpha$ and $\gamma$-CDs. Therefore, $\beta$-CD is easily crystallized, and is the most accessible and most generally used in the industry.

CDs are non-hygroscopic although their crystals contain water molecules. The contents of water in the crystals of α-CD, β-CD, and γ-CD are 10.2, 13.2-14.5, and 8.1-17.7 wt%, respectively. In the crystal state CDs produces relatively strong intermolecular hydrogen bonding which contributes to lower aqueous solubility of CDs as compared with other acyclic saccharides. The C-2 atom hydroxyl (OH) group of one glucopyranose unit can form a hydrogen bond with the C-3 atom OH group of the adjacent glucopyranose unit. A complete secondary belt is formed by these hydrogen bonds, which results in a relatively rigid β-CD structure, hence, imparting the lowest water solubility. The hydrogen bond belt is incomplete in α-CD, as one glucopyranose unit is in a distorted position. Hence, instead of six hydrogen bonds only four can be established. γ-CD has a non coplanar, more flexible structure, therefore, it has more solubility as compared to other CDs [4, 5, 6, 7].

## 1.4 Cyclodextrin Derivatives

CDs can be modified chemically in order to obtain a variety of derivatives with altered properties, such as increased or decreased aqueous solubility, and a significant effort has been focused on modifying the solubility of CDs. The solubility of CDs is usually dependent on the hydrophobic or hydrophilic nature of the modified groups, the degree of substitution, and the distribution of these groups on the CDs. The most commonly encountered and thoroughly studied derivatives are those of β-CD due to its large-scale commercial availability and relatively lower price than α and γ-CDs. Some examples of useful β-CD derivatives are listed in Table 2 [8, 9].

**Table 2.** Chemical structure and characteristics of β-CD derivatives

| Derivative | | Characteristics |
|---|---|---|
| **Hydrophillic** | | |
| Methylated β-CD | Me-β-CD | Solubility in cold water and organic solvent |
| | DM- β-CD | Hemolytic, surface active |
| Hydroxyalkylated β-CD | 2-HP- β-CD | Amorphous mixture |
| | 3-HP-β-CD | High water solubility, low toxicity |
| Branched β-CD | G1- β-CD | High water solubility |
| | G2- β-CD | Low toxicity |
| **Hydrophobic** | | |
| Alkylated β-CD | DE-β-CD | Water insoluble, surface active, soluble in organic solvent |
| Acylated β-CD | TA-β-CD | Water insoluble and soluble in organic solvent |
| | TV-β-CD | Film formation |

Abbreviations: Me: randomly methylated; DM: 2,6-di-O-methyl; 2-HP:2 hydroxypropyl; 3 -HP:3- hydroxypropyl; $G_1$:glycosyl; $G_2$: maltosyl; DE: valeryl; TA: 2,3,6 tri-O-acyl($C_2$-$C_{18}$); TV: 2,3,6 tri-O-valeryl.

## 1.5 Cyclodextrin Inclusion Complexes

One of the most important characteristics of CDs is their capability of forming inclusion complexes (ICs) with various compounds (guests) without involving covalent bonding. The terminology of inclusion complex was introduced in 1951 by Schlenk [10]. It is most frequently used in the literature although other names such as adduct, clathrate, etc. are sometimes used. The inclusion of a guest in a CD cavity is essentially a substitution of the included water molecules by the less polar guest. This process is an energetically favoured interaction of the relatively nonpolar guest molecules with an imperfectly solvated hydrophobic cavity as shown in Figure 2.

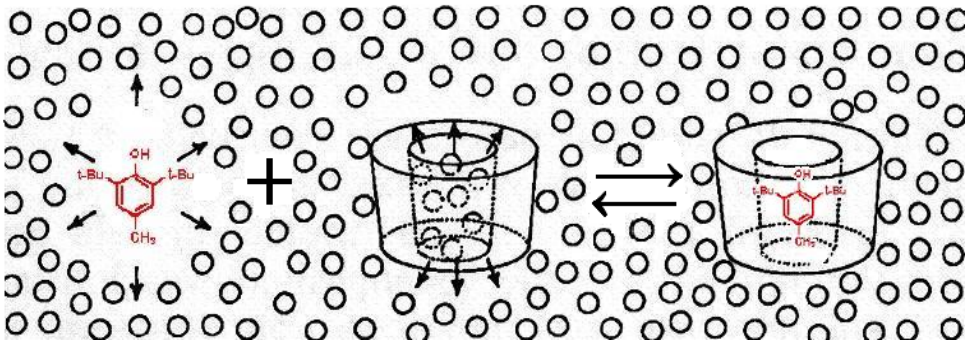


**Figure 2**. Inclusion complex formation

One of the basic requirements for complex formation is the geometric compatibility between the cavity of host CD and the guest molecule. As shown in Table 1, $\alpha$, $\beta$, and $\gamma$-CDs have cavities of increasing diameters, which may hold guest molecules of different sizes. For example, proprionic acid is compatible with $\alpha$-CD, but is rather

loosely fitted in the larger cavities of β and γ-CDs. Nevertheless, the complex formation does not require inclusion of the entire guest molecule in a CD cavity. A CD can complex with compounds that are significantly larger than its cavity by only including part of the guest molecules, for example, an hydrophobic side chain. Some guests will complex with more than one CD. The binding forces of a guest molecule, especially, low molecular weight guests, with the cavity of a CD involves several forces such as Van der Waals interactions, hydrophobic interactions, dipole-dipole interactions, and hydrogen bonding [11, 12].

CD inclusion complexes are either soluble or crystalline solids. There are two different forms of inclusion complexes in the crystalline state, channel and cage-type structures (Figure 3). Channel structures develop when CDs stack on top of one another to yield endless channels, in which long guest molecules, like polymers are included. Hence, the channel structure restricts only the lateral dimension of the molecules and places no restriction on the long dimension. The channel-type structure is further classified into two types, the head-to-head and the head-to-tail. Cage structures are different: both openings of the cavity are closed off by another CD, leaving the guest molecule entrapped in the cage. In the cage-type structures, CDs can be packed crosswise, in a herringbone fashion or in a brick-wall fashion [11].

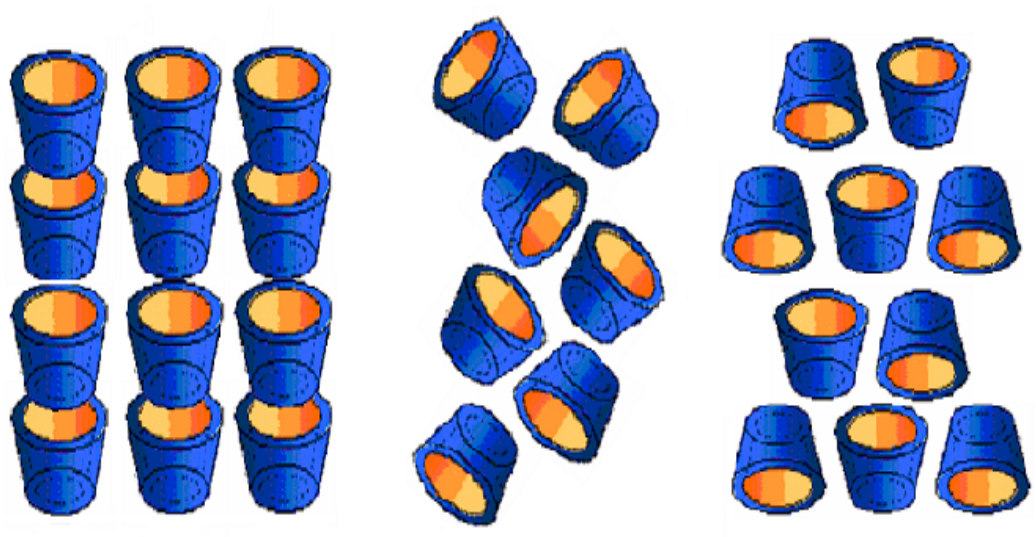

Channel (head to tail) Cage (Herringbone) Cage (Brick-wall)

**Figure 3.** Cyclodextrin inclusion complex crystal structures

### 1.5.1 Preparation of cyclodextrin inclusion complexes

The most commonly used methods are the co-precipitation, slurry, paste and dry mixing methods. They all are very similar except for the quantity of water used. Co-precipitation is most widely used in the laboratory. However, this method is not feasible for the large scale formation of complexes, because large amounts of water are used, which creates problem with the waste water disposal. The guest compound is added to the solution of cyclodextrin while stirring. The conditions are controlled in such a manner that the solubility of the complex is exceeded and the complex can then be collected as a precipitate by filtration as shown in Figure 4.

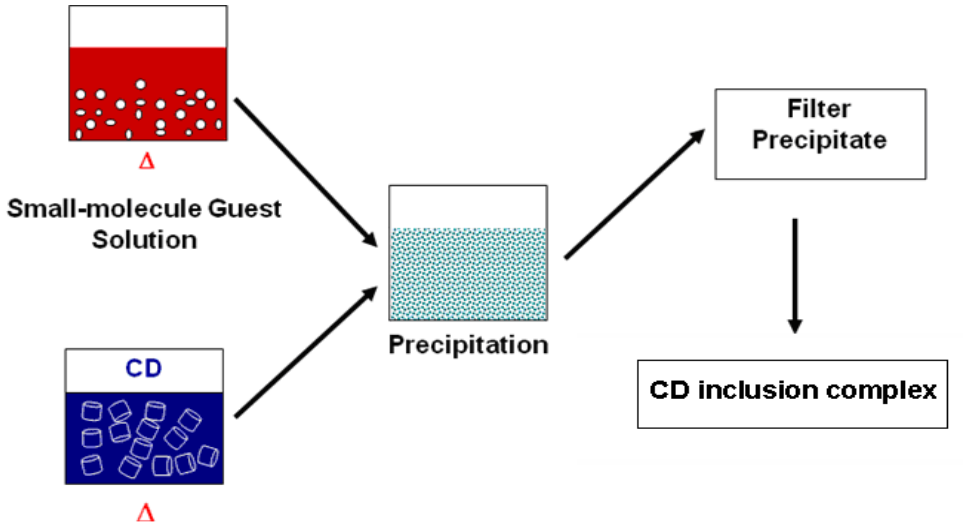


**Figure 4.** The co-precipitation method

In terms of the slurry method, CD is suspended in water at up to 40-45% w/w concentration. As the dissolved CD complexes with the guest and precipitates, more of the suspended CD dissolves to form more complex. Heating can be used if desired and if it is compatible with the guest. Then, the complex is collected by filtration and dried. In the paste method, CD, water and guest are added to a mixing device and mixed using a variety of mixers, such as extruders, blade mixers, kneading mixers, etc. This method utilizes a minimum amount of water (20-30% w/w). The mixing time varies with the guest to be complexed, amount of water, and the mixing device used. Generally a mixing device with high shear is preferred over those with lower shear, as it completes complexation in a shorter time. For the dry mixing method, CD is mixed with the guest in the absence of water. This is not an efficient method because mixing times can vary from hours to months. In some cases, guest can serve as a solvent for CD [6, 13].

### 1.5.2 Characterization of Cyclodextrin Inclusion Complexes

Various techniques such as differential scanning calorimetry (DSC), thermogravimetric analysis (TGA), nuclear magnetic resonance spectroscopy (NMR), wide-angle X-ray diffraction (WAXD), fourier transform infrared spectroscopy (FTIR), etc. can be used to analyze CD inclusion complexes. WAXD is used to confirm the crystal structures of CD complexes and DSC can be used to determine whether the inclusion compound contains free, uncomplexed guest. Since the guest is surrounded by the CD and does not interact with other guest molecules, there is no crystalline guest structure present to absorb energy, and no energy absorption is observed at the melting temperature of the guest molecules when the guest is complexed. Hence, the absence of the melting peak of guest molecules in the inclusion complex indicates that there are no free guest molecules. TGA can be used to measure the thermal stability and decomposition behavior of the inclusion complex.

A shift in peaks can be observed for both the host and the guest in soluble CD-ICs using NMR. As the environment around the hydrogen atoms in the CD cavity changes with association of the guest, a shift in the CD peaks for the complex can be observed. Similarly, shifts can be observed for peaks corresponding to the atoms of the guest which penetrates into the cavity of the CD. Also, NMR can be used for determining the stoichiometry of the inclusion complex. FTIR can be used for the analyses of CD complexes with peak shifts resulting in different spectra upon complexation of guests [3,13].

## 1.6 Applications of cyclodextrins

There are many applications of CDs for use in pharmaceuticals, foods, cosmetics, chemical industries, agriculture and environmental engineering as well as textiles. The CD inclusion complexation with guests can provide various advantages, such as preventing losses due to volatilization, oxidation, thermal degradation, and storage. For example, the CD inclusion compound containing menthol guests has a much more prolonged shelf life, compared with pure menthol at room temperature. The inclusion compound of CD with guest vitamin A palmitate increases its half-life against photo-degradation, while the pure vitamin degrades rapidly when exposed to light.

CD inclusion complexes are most widely used in the pharmaceutical industry. They can be used in drugs either for complexation or as auxilliary additives, such as carriers, diluents, solubilizers or tablet ingredients. Also, they may be used in foods and cosmetics to encapsulate flavors and fragrances. The application of CD inclusion complexes formed with food ingredients has many advantages: i) encapsulation of volatile oils and liquids for flavor protection, ii) elimination of undesired taste/odors, other undesired components, etc., and iii) protection of active food ingredients against oxidation, heat, and light. CD inclusion complexes can be also formed with a variety of agricultural chemicals such as herbicides, insecticides, fungicides, repellents etc. In the chemical industry, CDs can be widely used to isolate isomers and enantiomers, catalyze reactions, and to remove or to detoxify waste materials, etc. In textile industries, CDs are used to remove surfactants from

washed textiles, enhance dyeability of fabrics when chemically bound to fibers and for stabilizing dye molecules [13, 14, 15, 16, 17, 18, 19].

## 2. ANTIOXIDANTS

### 2. 1. Oxidative Degradation

Organic polymers can react with molecular oxygen in a process called autoxidation, initiated by heat, light (high-energy radiation), mechanical stress, catalyst residues, or reaction with impurities, to form alkyl radicals as indicated in Figure 5. The formed free radicals react in the presence of oxygen to form peroxy radicals, which further react with organic materials leading to hydroperoxides (ROOH). As these reactions proceed further, a great decrease in the molecular weight is observed due to chain scission originating at hydroperoxide groups. For example, the surface tackiness of some oxidized rubbers is the result of the decreased molecular weight due to the chain scission originating at the hydroperoxide groups as shown in the following reaction [20].

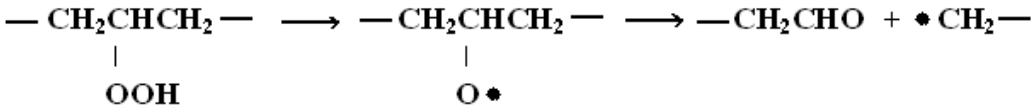

Also, it causes the polymer to degrade, resulting in embrittlement, melt flow instability, loss of tensile properties, and discolouration. Once oxidation starts, it sets off a chain reaction that accelerates degradation. However, oxidation can be

slowed to either reduce the rate of propagation by chain breaking antioxidants or inhibiting the initial formation of free radicals by antioxidant. Antioxidants deactivate the sites by decomposing the hydroperoxide or by terminating the free radical reaction. In general, antioxidants are added during polymer processing to protect polymers from oxidative degradation [21, 22, 23].

**Figure 5.** Oxidative degradation mechanism

## 2. 2 The Main Stages of Hydrocarbon Oxidation Reaction

The following mechanism of oxidation in liquid hydrocarbons is accepted as the appropriate one (Figure 5). This mechanism must, however, be applied with caution to the oxidation of solid materials such as polymers [21, 24, 25, 26].

## 2. 2.1 Chain Initiation

During the oxidation of a hydrocarbon the primary free radicals are formed as a result of a bimolecular or trimolecular reaction between the oxidized compound and oxygen. The rate of chain initiation reaction is slow, hence, it prevents a detailed study of the mechanism.

$RH + O_2 \rightarrow R\bullet + HO_2$ or $RH + O_2 + RH \rightarrow 2R\bullet + H_2O_2$

In some experiments, the chain initiation rate is enhanced by the addition of initiators such as peroxides or azo compounds.

$R\text{-}O\text{-}O\text{-}R \rightarrow 2RO\bullet \rightarrow R\bullet$ + products

$R\text{-}N \equiv N\text{-}R \rightarrow 2RO\bullet + N_2 \rightarrow R\bullet$ + products

## 2. 2. 2 Chain Propagation

The chain propagation stage of the hydrocarbon oxidation reaction includes two alternating reactions.

$R\bullet + O_2 \rightarrow RO_2\bullet$

$RO_2\bullet + RH \rightarrow ROOH + R\bullet$

## 2. 2. 3 Chain Branching

The degenerate branching of the chain of a hydrocarbon oxidation reaction occurs either through the monomolecular decomposition of hydroperoxide or bimolecular hydroperoxide reactions.

$ROOH \rightarrow RO\bullet + \bullet OH$ or $2ROOH \rightarrow ROO\bullet + RO\bullet + H_2O$

## 2. 2. 4 Chain Termination

In the absence of impurities, the chains ultimately terminate. Hence, the free radicals participating in the chain reaction decay by reacting with each other.

$2R\bullet \rightarrow R\text{-}R$

$R\bullet + ROO\bullet \rightarrow R\text{-}O\text{-}O\text{-}R$

$ROO\bullet + ROO\bullet \rightarrow RO + ROH + O_2$

## 2. 3 Types of Antioxidants

Antioxidants fall into two classes according to their mechanism for interrupting the degradation process: (i) chain terminating primary antioxidants and (ii) hydrogenperoxide decomposing secondary antioxidants [21, 22].

## 2. 3. 1 Primary antioxidants

Primary or free radical scavenging antioxidants inhibit oxidation via chain terminating reactions. The most important are sterically hindered phenolics and secondary aromatic amines. The hindered phenolic antioxidants are widely used through the plastic industry. They are effective during both processing and as long term thermal stabilizers. They behave as a free radical scavenger, which donates a hydrogen atom to a peroxide radical, thus, preventing propagation of the free radical chain reaction (Scheme 1). The efficiency can be enhanced by using them with other antioxidants such as phosphites and thioesters, producing synergistic effects for effective and economical formulations.

Scheme 1

ROO• radicals are deactivated by hindered phenol via the following reaction.

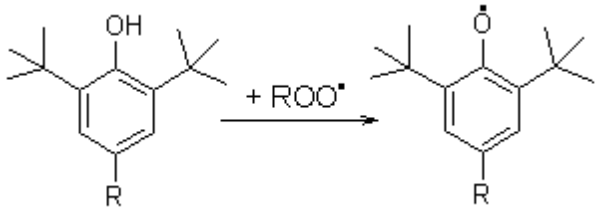

Butylated hydroxytoluene (BHT), as shown in Figure 6, is one of the phenolic antioxidants and its properties are listed in Table 3. It is primarily used as an antioxidant food additive, as well as in rubber, cosmetics, pharmaceuticals, jet fuels, and petroleum products. However, it is susceptible to loss through volatilization in high temperature applications [26, 27, 28].

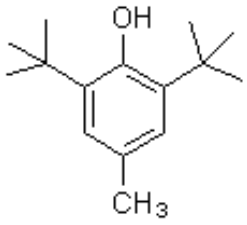


**Figure 6.** The chemical structure of BHT

**Table 3.** Physical and chemical properties of BHT

| Properties | BHT |
|---|---|
| Chemical Name | 3,5-di-tert-butyl-4-hydroxytoluene |
| Molecular formula | $C_{15}H_{24}O$ |
| Molar mass | 220.35 g/mol |
| Appearance | White powder |
| Solubility in Water | Insoluble |
| Melting point | 70-73°C |
| Boiling point | 265°C |

Secondary aromatic amines are often more active than hindered phenols, because they are sterically less hindered (Scheme 2). Aromatic amines, however, are more discoloring than hindered phenols, especially on exposure to light or combustion gases.

Scheme 2

ROO• radicals are deactivated by secondary aromatic amines via the following reaction.

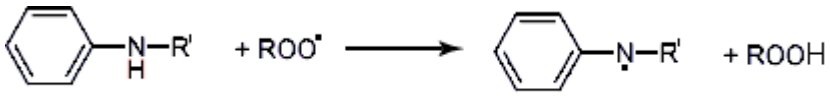


## 2. 3. 2 Secondary Antioxidants

Secondary antioxidants are referred to as hydroperoxide decomposers, because they decompose hydroperoxides into non-radical, non-reactive, and thermally stable products. They are often used in combination with primary antioxidants to yield synergistic stabilization effects and reduced color development during the lifetime of the plastics. The most important are organophosphorus compounds and thiosynergists. Organophosphorus compounds decompose peroxides and hydroperoxides into stable, non-radical products. Trivalent phosphorus compounds are excellent hydroperoxide decomposers. In general, phosphites (or phosphonites)

are used and they react according to the following general reaction, generating phosphates.

Scheme 3: Phosphites


Thiosynergists react according to the following general reaction, generating sulfoxides and sulfones.

Scheme 4: Thio-synergists

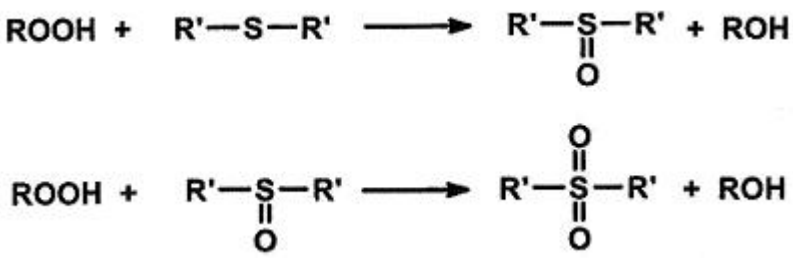


## 3. OXIDATION INDUCTION TIME/TEMPERATURE (OIT)

The OIT test can be performed with a differential scanning calorimetry (DSC) instrument for comparing the thermal stability of materials to oxidative attack. DSC is useful not only to help the researcher in developing effective additive systems for polymers, but also to aid them in evaluating whether a polymeric material has the expected processing properties and performance characteristics. The efficiency of these antioxidants can be analyzed using DSC under oxidation conditions by

calculating oxidation induction time ($OIT_{time}$) and oxidation induction temperature ($OIT_{temp.}$) from two measurement methods [29, 30, 31, 32]:

**Static OIT Method:** It measures $OIT_{time}$ of a given sample. It is a relative measure of a polymeric material's resistance to oxidative decomposition. Here the sample is heated in an inert atmosphere over its melting point to the selected temperature value. From this point, the temperature is held in the isothermal mode. Then, after reaching the equilibrium, the gas is switched to oxygen as shown in Figure 7. Finally the oxidation of the sample is observed as a sharp increase in the energy flow due to the exothermic nature of the oxidation reaction. Hence, $OIT_{time}$ is determined by the thermoanalytical measurement of the time interval to onset of exothermic oxidation of the material at a specific temperature in an oxygen atmosphere.

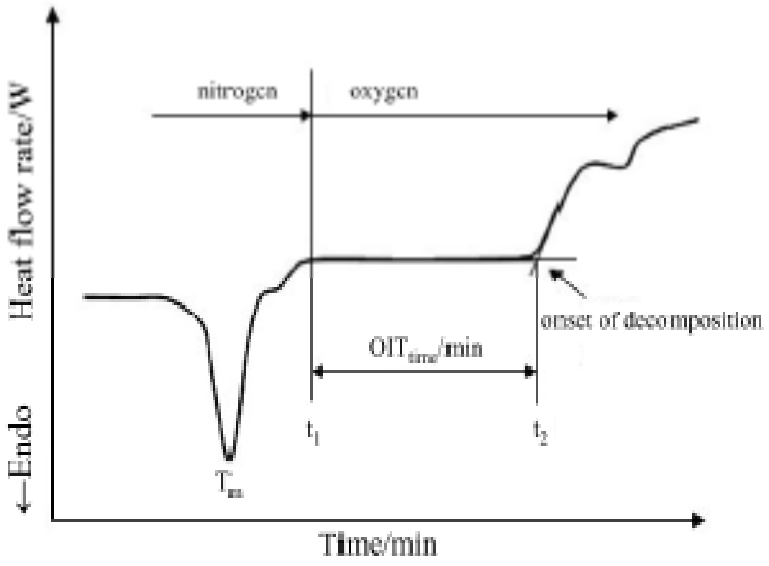


**Figure 7**. Principal sequence of $OIT_{time}$ according to ASTM D 3895-07 [29]

The most critical step in $OIT_{time}$ testing is determining a suitable temperature value for the isothermal phase. If the temperature value is too low then there is an increase in the $OIT_{time}$ measurement. If the temperature is too high, oxidation takes place immediately after the introduction of oxygen, and the onset of the temperature of decomposition can no longer be measured.

**Dynamic OIT method:** The $OIT_{temp.}$ is measured by heating the sample in air or oxygen at a linear heating rate . The oxidation of sample produces an exothermic curve as the energy is released.

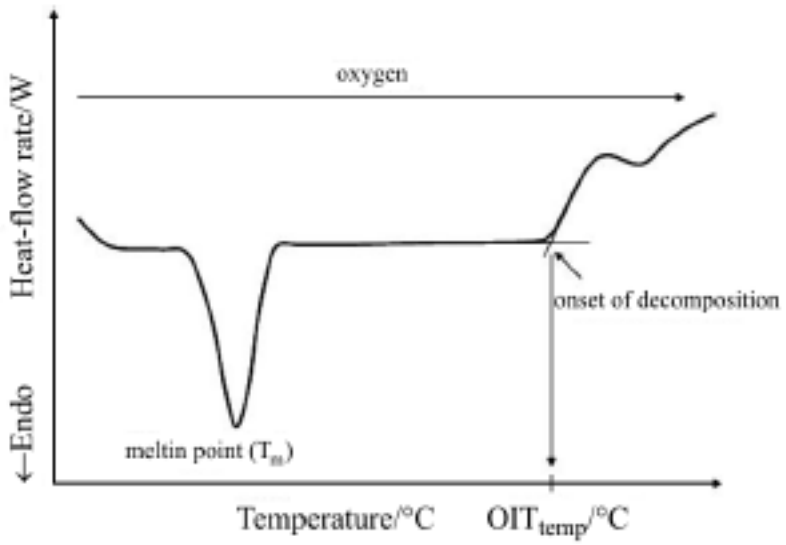


**Figure 8**. Principal sequence of $OIT_{temp.}$ according to ASTM D3895-07 [29]

Hence, the onset of oxidation temperature can be determined by analyzing the shift from baseline due to exothermic reaction. This method is simpler than the static method, as it does not involve a change of environmental gases. However, it is less sensitive as compared to the static method [30]. Also, this method has one major

limitation, as it cannot be used for comparing samples at high OIT temperature values, because the differences in the samples become indistinguishable. Therefore, $OIT_{temp.}$ method is good only for low $OIT_{temp.}$ values.

The largest application of thermal analysis is to investigate the behavior of stabilization systems, such as antioxidants in polymers like polyethylene. Polyethylene is a comparatively stable polymer, which finds application in films, pipes, mouldings, etc. However, one of the major drawbacks associated with polyethylene is its susceptibility to oxidative degradation during processing, storage, and use. Therefore, many researchers have conducted OIT measurement on polyolefin stabilized systems in the past. Schmid et al. [31] measured $OIT_{time}$ and $OIT_{temp.}$ on six different commercially available polyethylenes using DSC. Their results indicate that the determination of $OIT_{time}$ is associated with a high degree of uncertainty, especially for low $OIT_{time}$ values. Thus, $OIT_{temp.}$ measurement can be an alternative way for testing less stabilized or non-stabilized polyethylene. However, their results do not agree that the static OIT method offers higher sensitivity than dynamic OIT method, although it is more time-consuming. Also, the static method is normally used for quality control of polyolefin based polymers [30].

The effect of phenolic antioxidants (BHT and Irganox 1076 from Ciba-Geigy) and BHT transformation products (cyclohexadienone, benzoquinone, and stilbene-quinone) on the oxidative degradation of LDPE was examined using DSC combined with oxygen uptake measurements [33]. Their comparative study indicates a

pronounced stabilizing effect of stilbene-quinone in LDPE thermooxidation at about 90-100$^{o}$C. The effect of two commercial hindered piperidines antioxidants were compared to phenolic antioxidant BHT in LDPE film at 150$^{o}$C using DSC by Alfonso et al. [34]. Their results indicate that BHT was less efficient compared to other antioxidants. However, it is obvious that its $OIT_{time}$ was longer than virgin LDPE film. Bharel et al. [35] investigated the oxidation performance of two amide antioxidants by dry mixing them with fine HDPE powder. In addition, Breese et al [36] studied the oxidation induction time of various commercial hindered phenol antioxidants, including BHT in squalane, whose chemical structure is very similar to that of polypropylene. According to their comparison between Butylated hydroxyanisole (BHA) and BHT, BHA was a more efficient antioxidant than BHT. They also found that BHT has the lowest efficiency amongst various hindered phenolic antioxidants including the natural antioxidant, $\alpha$-tocopherol, in squalane. All these conclusions point to one major drawback of BHT, i.e. its high volatilization, which decreases its efficiency.

## 4. DYNAMIC MECHANICAL THERMAL ANALYSIS

Dynamic mechanical analysis (DMA) characterizes the mechanical and viscoelastic properties of polymers resulting from changes in five experimental variables: temperature, time, frequency, force, and strain. The storage modulus E' (elastic response) and loss modulus E'' (viscous response) of polymers are measured as a function of temperature or time as the polymer is deformed under an oscillatory load (stress) at a controlled (isothermal or programmed) temperature in a specified

atmosphere. The angle which reflects the time lag between the applied stress and strain is $\delta$, and a convenient dimensionless parameter is the loss tangent (tan $\delta$):

$$\tan \delta = E''/E'$$

The tan $\delta$ is a damping term and is a measure of the ratio of energy dissipated as heat to the energy stored in the material during one cycle of oscillation [36, 37, 38].

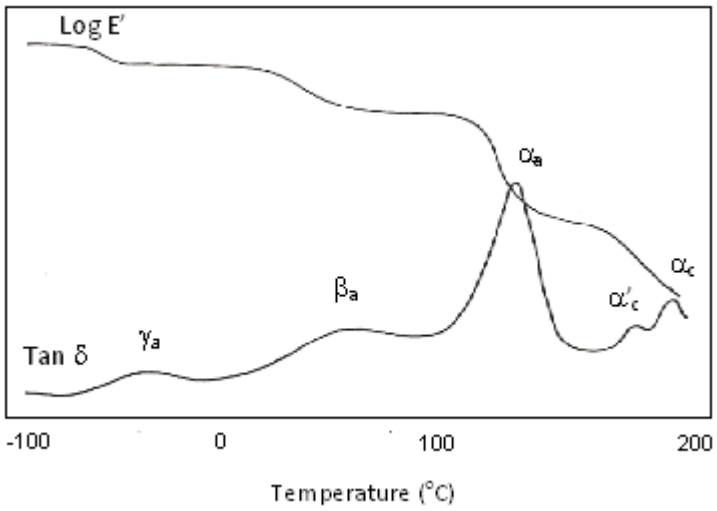


**Figure 9.** Typical transition behavior in mechanical storage modulus and damping for a semi-crystalline polymer. Subscripts a and c refer to the amorphous and crystalline phase, respectively [39]

In semi-crystalline polymers, relaxations can occur in crystalline regions as well as amorphous regions. Figure 9 illustrates the main features observed during a DMTA scan of a semi-crystalline polymer. Relaxation in the amorphous phase are denoted as $\alpha_a$, $\beta_a$, and $\gamma_a$, designated in alphabetic order as a function of decreasing temperature. The primary transition ($\alpha_a$) referred to as the glass transition ($T_g$),

which may be attributed to increased mobility of main polymeric chains, whereas the $\beta_a$ and $\gamma_a$ transitions may be accredited to either side group mobility and/ or end group motions of the main polymeric chains. Typically, the glass transition ($T_g$) is defined as the temperatures at which either a maxima of the damping parameter (tan $\delta$) or loss modulus (E'') occurs. Also, the onset of a sharp reduction in the storage modulus is referred to as the glass transition ($T_g$). Relaxations above $T_g$ in the crystalline phase are usually given the symbols $\alpha_c$', $\alpha_c$'', etc. in order of decreasing temperature [39, 40].

Dynamic mechanical studies of $\alpha$ and $\beta$ relaxations of polyethylene, a semi-crystalline thermoplastic polymer, were conducted by Popli et al. [41]. They described the α transition between 30 and 120ºC, the β transition in the range of

$-$ 30 to 10ºC, and γ transition in the range $-150$ to $-120$ºC. The α relaxation is caused by the segmental motion of chain molecules which exists within the crystalline portion of polymer. Upon the incorporation of structural and chemical factors into the chain, such as branching, adding fillers, plasticizers, copolymerization etc., the crystallinity level reduces and this decreases the intensity of the α transition. The β relaxation in some of the linear polyethylenes has not been detected [42, 43, 44] or barely found [45, 46]. On the contrary the β relaxation for branched polyethylene and ethylene copolymers is known and it depends on branching level and thus apparently the degree of crystallinity [47, 48].

Thermomechanical analysis of CD inclusion complexes with antioxidant by DMTA in films has rarely been the focus of research. There is only one peer reviewed research paper regarding dynamic mechanical thermal analysis of CD inclusion complex films [49]. The authors found that the storage modulus profiles of the α-CD inclusion complex films with poly(ε-caprolactone) show significant increases as compared with that of the pure poly(ε-caprolactone) films. In addition, the storage modulus of the inclusion complex films increases with an increase in the number of α-CD molecules threaded on the poly(ε-caprolactone) chains. The tan δ peak shifts to a higher temperature region by forming the inclusion complex. Further, the tan δ peaks of the inclusion complex become broad compared to the pure poly(ε-caprolactone). It indicates that the poly(ε-caprolactone) chain has a broad range of mobility in the inclusion complex state. In addition, thermal stability of the inclusion complex films increases over 150$^{o}$C as compared with the melting of the pure poly(ε-caprolactone) film at about 60$^{o}$C.

As mentioned above, relatively little research has been conducted on CD inclusion complex films. However, much research has been done to investigate the effect of starch on thermal properties of LDPE films using DMTA. Jagannath et al. [50] measured the thermal properties of LDPE film with different quantities of starch using DMTA. They found that glass transition temperature ($T_g$) decreased with an increase in starch content in the LDPE film. Pedroso and Rosa [51] studied the viscoelastic behavior of the LDPE film with an increase in corn starch content using

DMTA. The addition of starch to LDPE film caused the storage modulus values to increase since starch decreases the polymer chain mobility. In general, the addition of starch caused a shift in the maxima of loss modulus to higher temperatures. Also, the peaks where tan $\delta$ was maximum, broadened and shifted to lower temperatures when starch was added to LDPE film.

# 5 MOTIVATION

Cyclodextrin (CD) inclusion complex (IC) formation with various active components is an important characteristic of CDs. One of the many applications of ICs is to prevent losses of volatile active components due to volatilization. The phenolic antioxidant, BHT, is primary used as an antioxidant food additive, but BHT is highly volatile. Therefore, it is susceptible to loss through volatilization during processing. Hence, by forming CDs-IC with BHT, volatilization of BHT can be greatly reduced during polymer processing, providing more stable delivery to polymers. However, there is barely any research work focused on the formation of BHT-CD-ICs [52, 53]. BHT is primarily used as a food antioxidant in many packaging materials, which are made from low density polyethylene (LDPE) and polypropylene. In addition, LDPE is susceptible to oxidative degradation during processing. Hence, LDPE was selected in this study. Furthermore, the production of the films with the BHT-$\beta$CD-IC was shifted from lab scale to pilot production, leading to greater potential applications in the consumer market.

In terms of characterization of the films, no literature work is present on CD-IC oxidation induction time and/or temperature (OIT) measurements. Hence, OIT study was chosen. We found only one peer review paper on characterizing CD-IC using dynamic mechanical analyzer (DMA). Hence, DMA analysis is also studied.

# II. EXPERIMENTAL

## 1. MATERIALS

Food-grade β-CD and synthetic phenolic antioxidant BHT were obtained from Wacker Chemicals and Ciba Specialty Chemicals, respectively. Chloroform, dimethylformamide (DMF) and dimethyl sulfoxide-$d_6$ (DMSO-$d_6$) were purchased from Sigma Chemical Co., USA and used as supplied. In addition, low-density polyethylene (LDPE) chips were obtained from Plastics Color Corporation, NC, USA.

## 2. PREPARATION OF BHT-β-CD-IC

Small-scale BHT-β-CD-IC was prepared by the slow and drop wise addition of 0.1g of BHT dissolved in chloroform (2 ml) to 11.0 mL of an aqueous solution with 1.00 g of β-CD held at 60$^{o}$ C. As the BHT solution was added, a white turbid solution was formed. After stirring it continuously for 3 hours at 60ºC, the covered flask was removed from the hot plate. Then, the white precipitate solution was left unperturbed overnight. The white precipitate was collected by filtration and the crystals were washed with distilled water and air-dried. The small-scale inclusion

complex was characterized using DSC, TGA, NMR and WAXD. For large-scale inclusion complex for extrusion of films on pilot scale, the small-scale method was used except that 2g of BHT dissolved in chloroform (40 ml) was added to 220 mL of an aqueous solution with 20.00 g of β-CD. The amount of BHT included in the complex from the large-scale was characterized using UV-Vis Spectroscopy.

## 3. CHARACTERIZATION OF BHT-β-CD-IC

### 3. 1 Wide-Angle X-ray Diffraction (WAXD)

Wide-angle X-ray diffraction (WAXD) measurements were performed with a Siemens type-F X-ray diffractometer using a Ni- filtered CuKα radiation source (λ =1.54 Aº). The diffraction intensities were measured every 0.1º from 2Θ = 10 to 30º at scanning speed of 2Θ= 5º/min. The supplied voltage and current were 30kV and 20 mA, respectively.

### 3. 2 Differential Scanning Calorimetry (DSC)

Differential Scanning Calorimetry (DSC) experiments were carried out on 3-10 mg samples with a Perkin-Elmer DSC 7 under nitrogen purge gas. BHT and BHT-β-CD-IC samples were heated at a heating rate of 20$^{o}$C/ min from 25 - 100ºC and 25-250ºC, respectively. The software used to analyze these DSC scan was Pyris series version 5.00.02.

## 3. 3 Thermogravimetric Analyzer(TGA)

TGA scans of as received β-CD, BHT and BHT-β-CD-IC were obtained with a Perkin Elmer Pyris1 thermogravimetric analyzer. Samples weighing 8-10 mg were placed in an open platinum pan that was hung in the furnace. The weight percentage of remaining material in the pan was recorded during heating from 25 to 600$^{o}$ C at a heating rate of 30$^{o}$ C/min. Nitrogen was used as the purge gas.

## 3. 4 Nuclear Magnetic Resonance Spectroscopy (NMR)

$^{1}$H NMR solution spectra of BHT and BHT-β-CD-IC dissolved in DMSO-$d_6$ were recorded on a Bruker Avance 300MHz spectrometer in DMSO-$d_6$. One dimensional $^{1}$H data sets contained 16k data points and scans sufficient to obtain good S/N were collected.

## 3. 5 UV-VIS Spectroscopy - Quantitative analysis

For establishing a calibration curve, the stock solution was prepared by dissolving BHT (13.2 mg) in 100 mL dimethylformamide (DMF). Then, five standard solutions were prepared from the stock solution, the absorbances of the solutions was measured, and a calibration curve was obtained. The amount of BHT included in the complex was quantified by the following method: A total of 9.80 mg complex was dissolved in 5 ml of DMF and the absorbance was measured at 278 nm, which is the maximum absorbance peak of BHT, by Ultraviolet Visible (UV-VIS)

Spectroscopy (Cary 3E, Varian, Inc. USA). The concentration of BHT in the complex was obtained from the calibration curve.

## 3. 6 TGA Analysis of BHT release from its β-CD-IC

The release of BHT from its β-CD-IC was measured on a Perkin-Elmer Pyris1 thermogravimetric analyzer. Samples weighing 5-10 mg were placed in an open platinum pan that was hung in the furnace and the samples were heated at 20ºC/min and maintained at 110ºC over a 120 min period. The weight percentage of remaining material in the pan at various times at 110$^{o}$ C was recorded in a nitrogen atmosphere.

## 4. EXTRUSION OF FILMS

Low-density polyethylene (LDPE) chips were obtained from Plastics Color Corporation, who also compounded three sets of the polymer chip (4536 g) with (a) the BHT (9 g), (b) large-scale BHT-β-CD-IC (171 g of β-CD and 9 g of BHT ), and (c) β-CD (171 g). The LDPE, BHT LDPE, β-CD LDPE, and BHT-β-CD-IC LDPE films were prepared from the compounded chips by a single screw film casting extruder (Killion Film Extruders, USA) at the Clemson Packaging Center.

## 4. 1 Film Characterization

### 4. 1. 1 GC-MS - Quantitative Analysis

2.0 g film was accurately weighed and cut into small pieces. The BHT in the BHT-LDPE film and BHT-β-CD-IC LDPE film was extracted using the standard AATCC Test Method, 95-1995, "Extractable Content of Greige and/or Prepared Textiles" with some modifications. After Soxhlet extraction, the solution was filtered through a filter paper. The solvents were evaporated to dryness in a rotary evaporator (Model RE121, Buchi Corporation) at 50$^{o}$C. The amount of BHT obtained from the LDPE film extracts was quantified by Gas chromatography-Mass Spectrometry (GC-MS, Hewlett Packard, USA). Separation was performed on 30x0.32 mm internal diameter 50% phenyl-50% methyl polysiloxane column (Restek Corporation, USA). One (1) μl samples are injected into the injector port where they are vaporized and carried into the column by the carrier gas, helium, at a flow rate of 1 ml/min.

For quantification purposes, eicosane (Sigma Chemical Co., USA) was added to the samples. Eicosane was chosen to serve as an internal standard, since physical properties of eicosane are similar to those of BHT. BHT concentration of the films was determined from standard graphs constructed by analyzing BHT using eicosane as standard. For constructing standard graphs, a series of BHT standard solutions containing 15 ug eicosane/mL in heptane was prepared as indicated in Table 4.

**Table 4**. BHT standard concentrations

| Sample | BHT |
|---|---|
| Standard 1 | 5 ug/ mL in heptane |
| Standard 2 | 10 ug/ mL in heptane |
| Standard 3 | 30 ug/ mL in heptane |
| Standard 4 | 50 ug/ mL in heptane |

## 4. 1. 2 Morphology

Microscopy studies were done on LDPE film, β-CD LDPE film and β-CD-BHT-IC LDPE film using SMZ-1000 stereo microscope in transmission mode. The samples were placed on the glass slide of the microscope. The optical micrographs were captured using Nikon DS-F1 digital camera surmounted on the instrument. The software version used was NIS Elements F 2.20.

## 4. 1. 3 Oxidation Induction Time/Temperature Measurement

**Instrument calibration:** A two point calibration step was done using Zinc and Indium as the calibrants. 2 ± 0.5 mg of zinc/indium was placed into an aluminum sample pan and then was sealed. An empty sealed reference pan to be used as reference was prepared. Both the pans were placed in their respective positions in the instrument. Oxygen gas was turned on at the flow rate of 60 cc / min. Then, the following melting profile was used:

Zinc= heating from 380 – 450º C at 10 ºC/min

Indium= heating from 120 -170º C at 10º C/min.

Now the temperature calibration software was adjusted to set their respective melting points.

**Oxygen Induction Time ($OIT_{time}$) measurement:**

The $OIT_{time}$ testing was performed using a method based on ASTM D 3895-07 " Oxidative Induction time of Polyolefins by Differential Scanning Calorimetry". The instrument used was a Perkin Elmer DSC 7 with Pyris software version 5. Initially the sample (5-6 mg) was held for 5 min at ambient temperature (25ºC) under a flow of nitrogen gas (55cc/min). This was followed by heating to 190ºC at the rate of 20ºC/min, still under the flow of nitrogen. After reaching 190ºC, the sample was held for a further 5 min, after which the gas was switched from nitrogen to oxygen (60cc/min). This changeover point to oxygen flow is considered the zero time of the experiment. Then, isothermal operation was continued to analyze the complete sample until the maximum exotherm is reached. Upon completion of the test, gas was switched again to nitrogen and the instrument was cooled to ambient temperature. The sample holders (aluminum pans) were covered by the lid while performing the DSC scans.

**Oxygen Induction Temperature ($OIT_{temp.}$) measurement:**

The sample (5-6 mg) is heated up continuously from ambient temperature (25ºC) until the oxidation of the material was seen as an exothermic peak under pure oxygen atmosphere (60cc/min) at the heating rate of 10ºC/min. The sample was kept in aluminum pan and was covered by the lid while performing the DSC scans.

## 4. 1. 4 Dynamic Mechanical Thermal Analysis

Dynamic mechanical properties of LDPE film and LDPE films containing BHT, β-CD, and β-CD inclusion complex with BHT were studied using a dynamic mechanical analyzer, model Q 800 (Texas Instrument, USA). The DMA equipment was calibrated according to the recommended procedures using the manufacturer's software. The storage modulus *(E'),* loss modulus (*E''*)**,** and loss tangent (tan δ**)** were obtained in a tension film multifrequency controlled stress configuration suited for the semicrystalline thermoplastic polymer samples. These properties were measured at a frequency of 1Hz and over the temperature range of – 40 to 110$^{o}$C with a heating rate of 5$^{o}$C/min. The test specimens were 30.28 X 6.25 X 0.11 mm (length, width, thickness).

# III. RESULTS AND DISUSSION

## 1. CHARACTERIZATION OF BHT-β-CD-IC

### 1. 1 Wide-Angle X-ray Diffraction (WAXD)

Figure 10 shows the wide-angle X-ray patters observed for β-CD, BHT, and small scale BHT-β-CD-IC. By comparing the diffraction pattern of BHT-β-CD-IC with that of β-CD, the most intense peak of β-CD in the position of $2\theta = 12.8^{o}$, which has been proved to be a cage structure [54], also appears in BHT-β-CD-IC. It may be concluded that little or no change was made in the cage structure of β-CD after formation of inclusion complex. Also, the most intense peak in the diffraction pattern of the inclusion complex showed in the position $2\theta = 22.7^{o}$, while the most intense peak in the diffraction pattern of BHT was in the position of $2\theta = 20.6^{o}$. This also may indicate the formation of inclusion complex between BHT and β-CD. However, further study of BHT-β-CD-IC may be needed because of its complicated diffraction pattern.

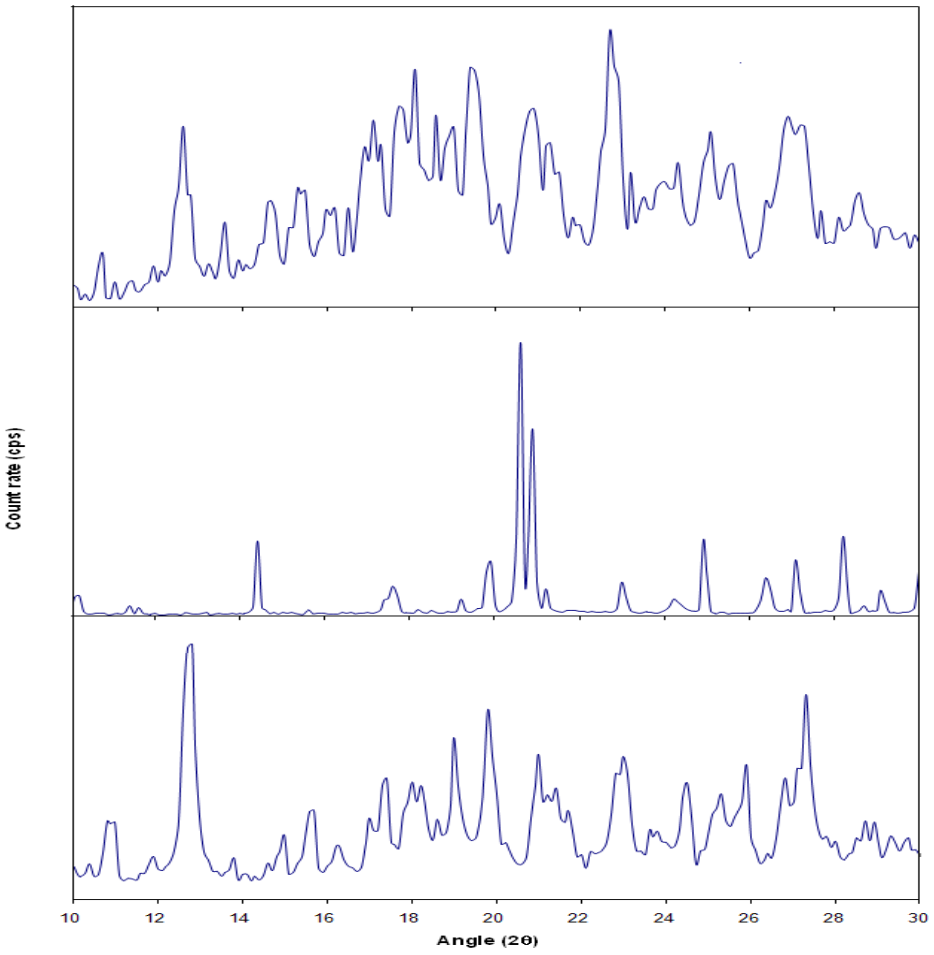


**Figure 10.** X-ray diffraction patterns of β-CD (bottom), BHT (middle) and BHT-β-CD-IC (top)

## 1.2 Differential Scanning Calorimetry (DSC)

The DSC technique was employed to determine whether the inclusion compound obtained contained free, uncomplexed BHT guest. As seen from the figure 11, the melting peak of pure BHT is at 70ºC. When BHT is complexed, it is surrounded by the cyclodextrin molecules, thereby preventing interactions with other BHT molecules. Hence, the absence of a BHT melting peak in the heating scan of β-CD-

BHT-IC indicates that BHT-β-CD-IC contains no free uncomplexed BHT. Also, an endothermic peak of BHT in the physical mixtures of β-CD and BHT, which has the same molar ratio of the inclusion complex in small-scale, was observed at about 70ºC, indicating the presence of BHT in the physical mixtures. Hence, this further confirms the formation of BHT-β-CD-IC. In addition, in the heating scan of BHT-β-CD-IC and the physical mixtures endothermic peaks appear at about 182ºC and 195 ºC, which indicates the dehydration of water molecule in the β-CD molecule.

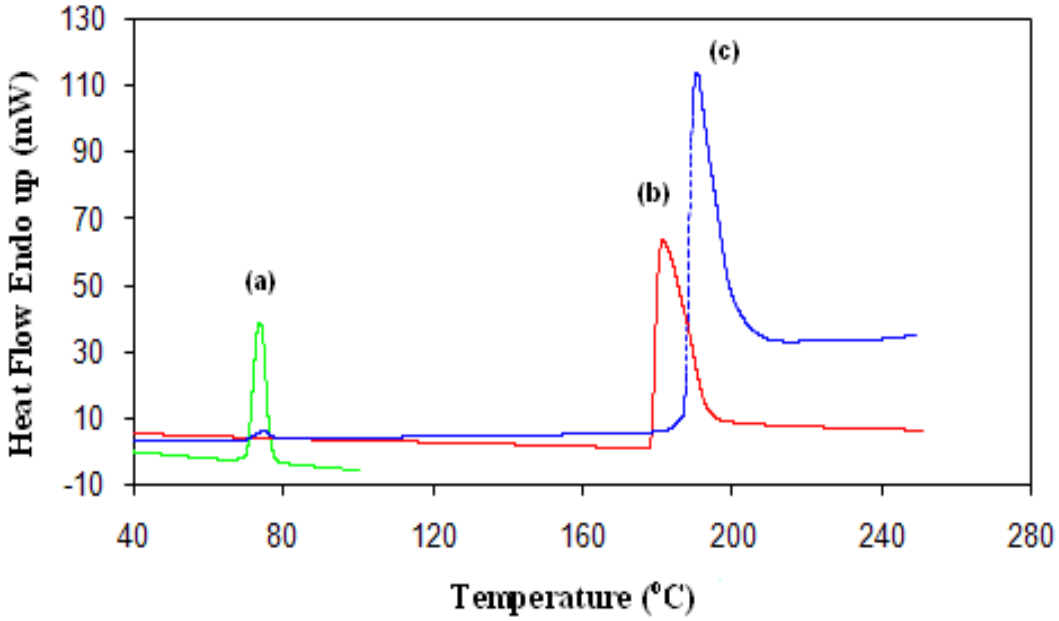


**Figure 11.** DSC scans of (a) BHT, (b) small scale BHT-β-CD-IC, and (c) the physical mixtures of β-CD and BHT(molar ratio of β-CD:BHT= 2:1)

## 1. 3 Thermogravimetric Analyzer(TGA)

TGA was used to measure the thermal stability and decomposition behavior of β-CD, BHT, and BHT-β-CD-IC, as shown in Figure 12.

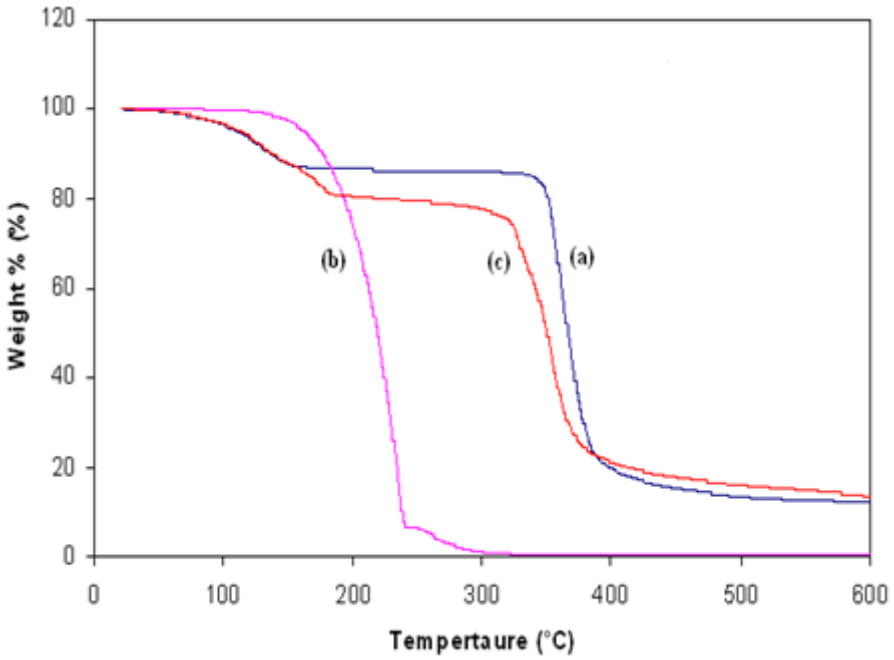


**Figure 12**. TGA scans of (a) β-CD, (b) BHT and (c) small scale BHT-β-CD-IC

Figure 12 shows that BHT-β-CD-IC has a higher decomposition temperature as compared with pure BHT. In addition, the decomposition temperature of BHT-β-CD-IC is consistent with the β-CD sample. Hence, the formation of inclusion complex prevents loss of BHT as well as improves the thermal stability of BHT. Due to high volatility of BHT, its first step corresponds to main chemical degradation of the BHT where maximum weight loss takes place at 238ºC. In addition, small second stage is observed which may be due to the degradation of residue. In terms of β-CD, the

first step is due to the loss of absorbed water and water of crystallization. The second stage where the maximum weight loss occurs (~ 70-80%), is associated with the formation of a residue (char) in the temperature range of 250-400ºC. The last stage is basically slow thermal degradation of char [55]. On the other hand, BHT-β-CD-IC shows a profile similar to β-CD, where the whole process takes place in three stages, namely in the first stage removal of water, second major weight loss due to the chemical degradation at about 354 ºC and finally the degradation of the residue.

## 1. 4 Nuclear Magnetic Resonance Spectroscopy (NMR)

Further confirmation of the formation of an inclusion complex was observed in the $^{1}H$ NMR spectra of small scale BHT-β-CD-IC and BHT dissolved in DMSO-$d_6$, as shown in Figure 13. In the proton spectra of BHT and BHT-β-CD-IC at about 2.5 ppm is from DMSO-$d_6$. The peak corresponding to eighteen(18) t-butyl methyl protons of BHT was identified at about 1.35 ppm. The peaks of BHT at about 2.2 ppm, 6.65 ppm, and 6.85 ppm were due to three protons of the p-methyl group, protons of the phenyl group, and the –OH proton, respectively. The protons peaks on the C-1, C-2, C-3 C-4, C-5, and C-6 of the β-CD in the complex were identified at about 4.82, 5.71, 5.67, 4.45, 3.63 and 3.54 ppm, respectively. The assignment of the β-CD protons were also confirmed [56]. New proton resonances in the inclusion complex spectra at about 1.35 ppm, 2.2 ppm, 6.65 ppm and 6.85 ppm are contributed by BHT. Therefore, it confirms the presence of BHT in the BHT- β-CD-IC sample. The stoichiometry of the inclusion complex is obtained directly from the

$^1$H NMR spectrum of BHT-β-CD-IC by integrating and comparing the areas of resonance peaks contributed by BHT and β-CD. It was found that β-CD forms a 2:1 inclusion complex with BH in the case of the small-scale inclusion complex.

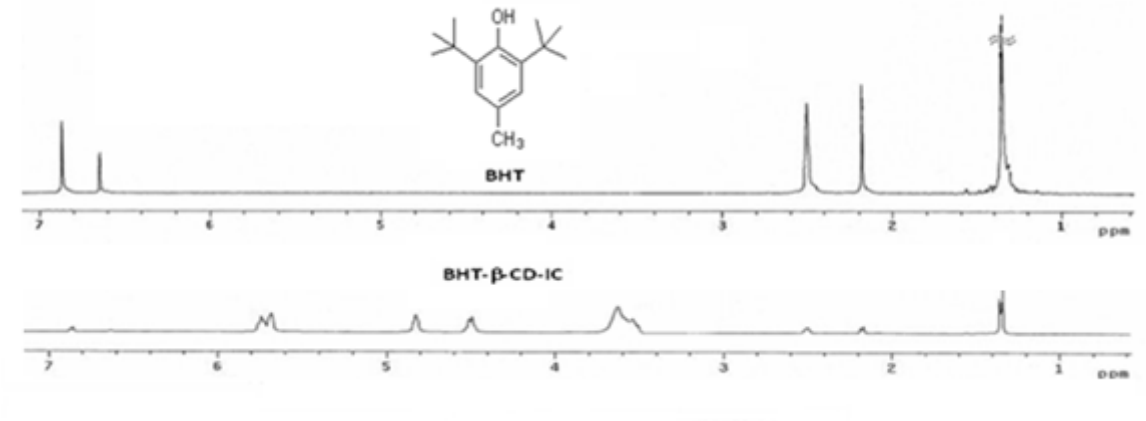


**Figure 13.** $^1$H NMR spectra of BHT and BHT-β-CD-IC.

## 1. 5 Quantitative analysis of BHT in the inclusion complex

The concentration of BHT for the large-scale inclusion complex was determined using UV-Vis Spectroscopy. The calibration curve was constructed from the absorbance of standard solutions as shown in Figure 14.

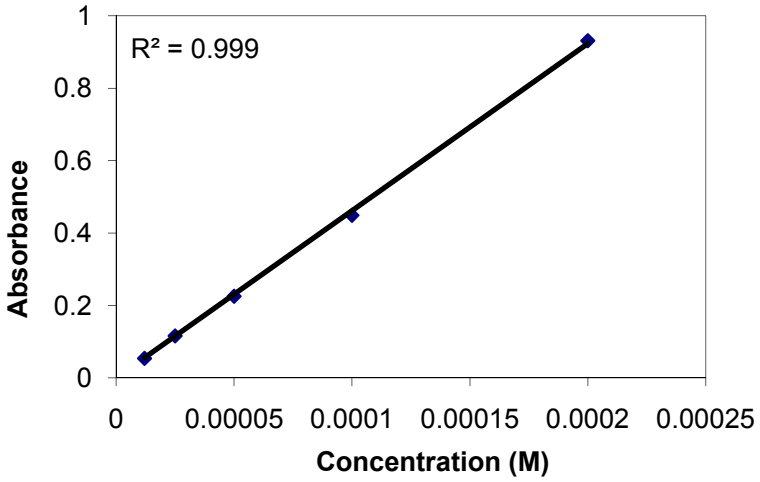


**Figure 14.** Calibration curve obtained from BHT ($\lambda_{max}$ = 278 nm) standards

Beer 's law is a linear relationship between absorbance and concentration, given by

$$A = a*b*c$$

where A= absorbance, c = concentration, b= pathlength and a= molar absorptivity.

Beer lambert's law was used to determine the concentration of BHT in the inclusion complex. After measuring the absorbance of the unknown concentration of BHT in the inclusion complex as shown in Figure 15, the concentration of BHT in the complex was obtained from the calibration curve. It was found that the concentration of BHT in 10 mg of inclusion complex is 0.5 mg, indicating that β-CD forms about 4:1 inclusion complex with BHT in the case of large-scale inclusion complex.

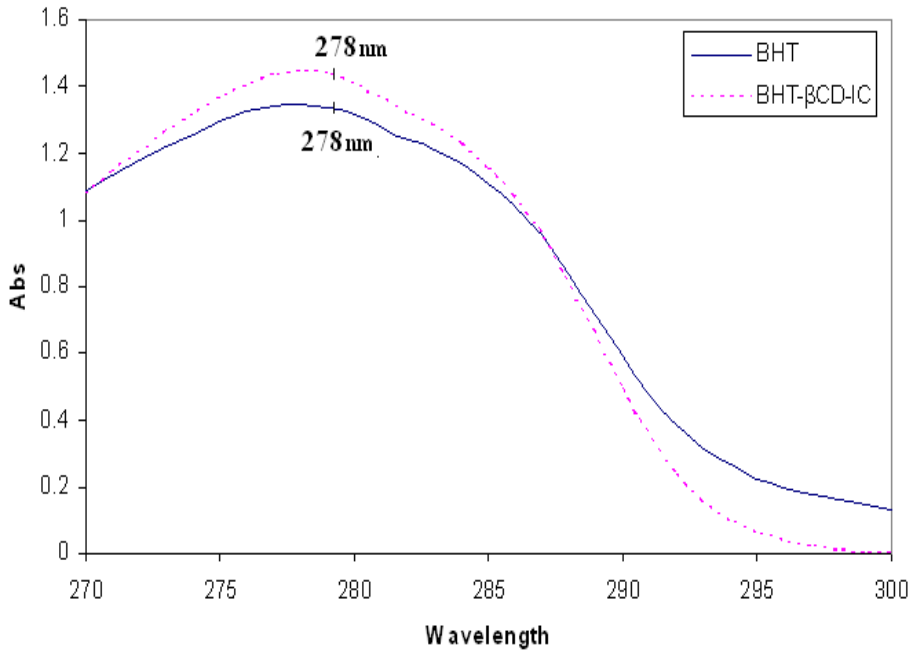


**Figure 15.** UV-Vis spectra of BHT and β-CD-BHT-IC

## 1.6 TGA Analysis of BHT release from its β-CD-IC

The release characteristics of BHT from the small-scale inclusion complex as well as pure BHT was determined by measuring percent weight loss at 110$^{o}$C over 120 min. period, as illustrated in Figure 16. The continuous weight loss is observed in BHT sample over a period of time and complete weight loss occurs at about 77 min because of its high volatility. On the contrary in the case of BHT-β-CD-IC, minor weight loss changes are observed after about 20 % weight loss at about 30 min. However, TGA may not be a good tool for measuring the BHT release characteristics of the BHT guest in the inclusion complex without knowing how much moisture is included in the complex.

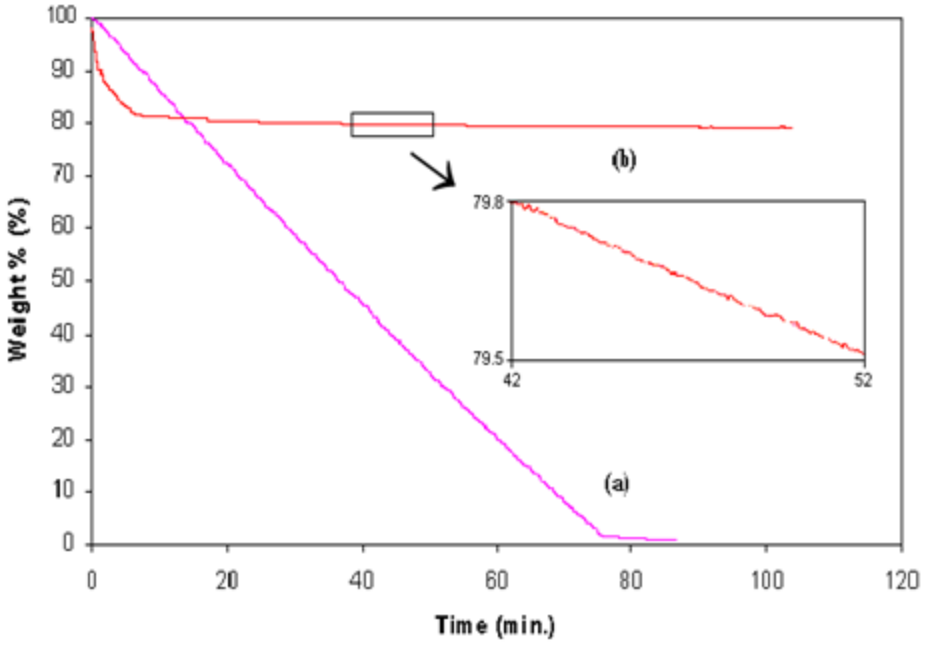


**Figure 16.** TGA scans of (a) BHT and (b) BHT-β-CD-IC

## 2. LDPE FILM CHARACTERIZATION

### 2. 1 GC-MS Quantitative Analysis

A calibration graph was constructed in which the ratio of the peak areas of the standard BHT concentration to that of the internal standard is plotted on the y-axis versus the concentration of the BHT on the x-axis. Figure 17 shows the calibration curves constructed from the peak areas as shown in Table 5. The retention times of BHT and eicosane are at about 9.7 min and 12 min, respectively, as shown in Figure 18.

**Table 5**. The peak areas of the standard BHT concentrations

| BHT (ug/mL) | Area response | Eicosane (ug/mL) | Area response | Normalized response |
|---|---|---|---|---|
| 5 | 1,0752,626 | 15 | 38,983,436 | 0.28 |
| 10 | 36,262,171 | 15 | 69,523,680 | 0.52 |
| 30 | 63,683,455 | 15 | 35,932,378 | 1.77 |
| 50 | 123,602,372 | 15 | 39,157,268 | 3.16 |

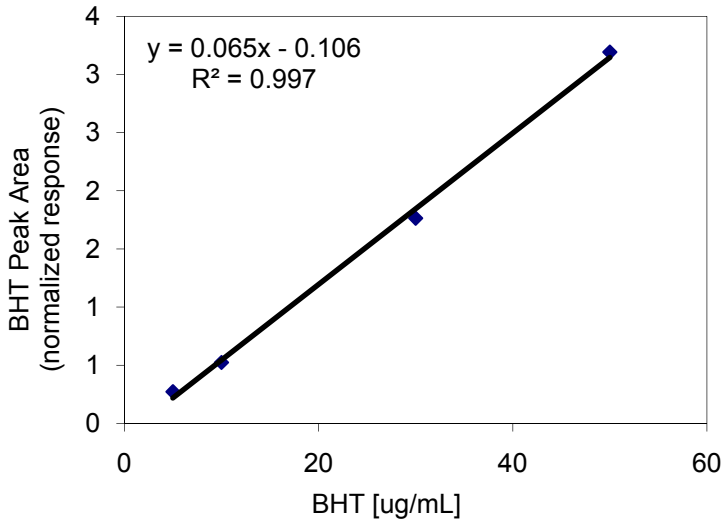


**Figure 17.** The calibration graph constructed from the BHT standard solutions

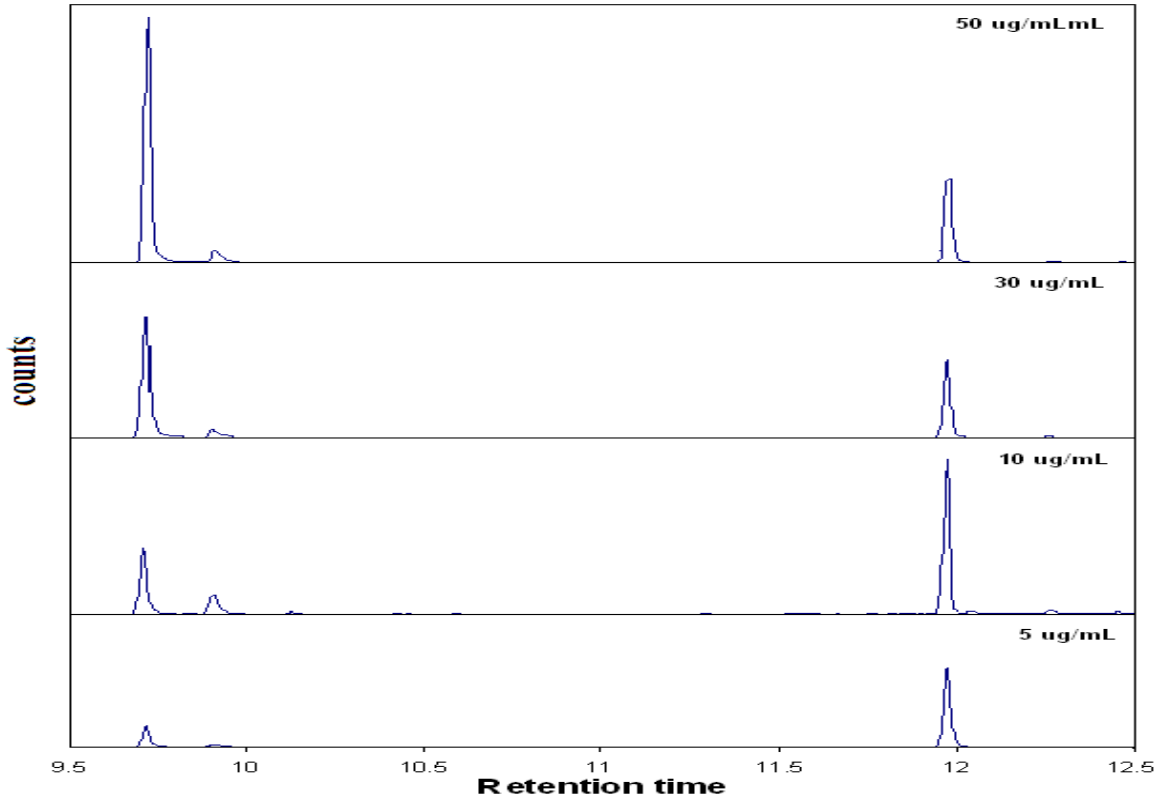


**Figure 18.** GC chromatogram of the BHT standard solutions

From the calibration curve, as shown in Figure 17, the initial BHT concentration in the BHT LDPE and BHT-β-CD-IC LDPE films after extrusion were determined. Figure 19 shows GC chromatograms of the film extracts. Initially before extrusion, BHT LDPE film and BHT-β-CD-IC LDPE film contain approximately 3968 μg of BHT/2g of the films. After extrusion, the BHT contents of the BHT LDPE film and BHT-β-CD-IC LDPE film were 858 μg/2g and 2235 μg/2g, respectively according to the results indicated by GC-MS. Therefore, there was about 78 and 44% loss of BHT from the extruded BHT LDPE film and BHT-β-CD-IC LDPE film, respectively.

Hence, the cyclodextrin inclusion complex LDPE film proved to be more efficient in preventing loss of BHT from the extrusion.

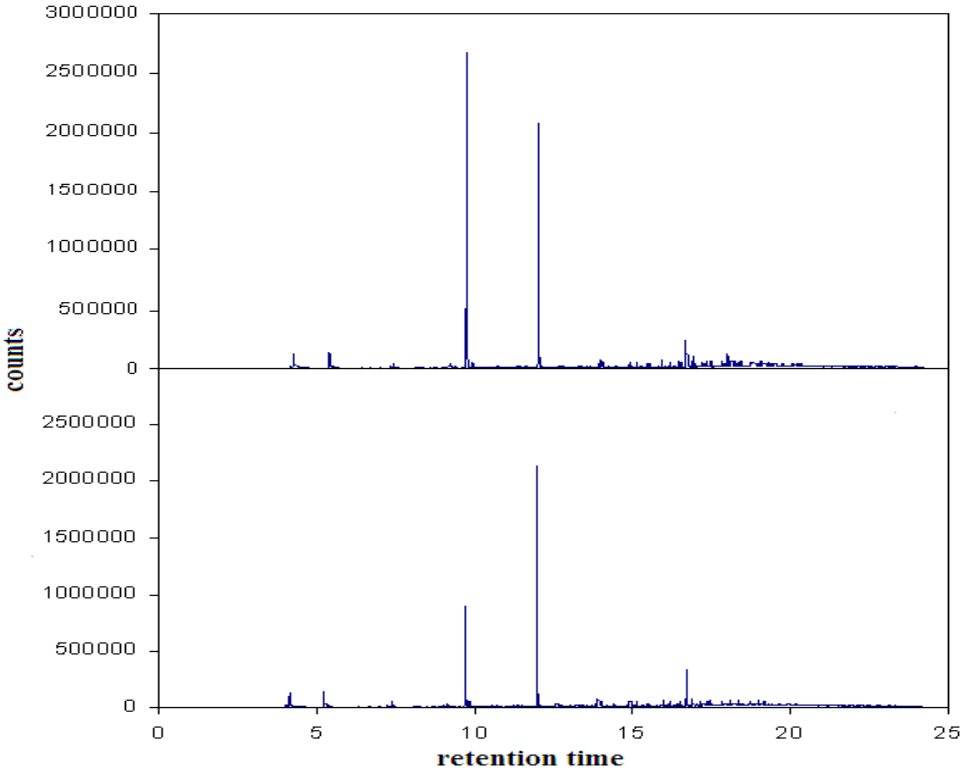


**Figure 19**. GC chromatograms of the BHT- β-CD-IC LDPE film (top) and BHT LDPE film (bottom)

## 2. 2 Morphology

Figure 20 shows the microscopic photos of LDPE film, β-CD LDPE film and BHT-β-CD-IC LDPE film.

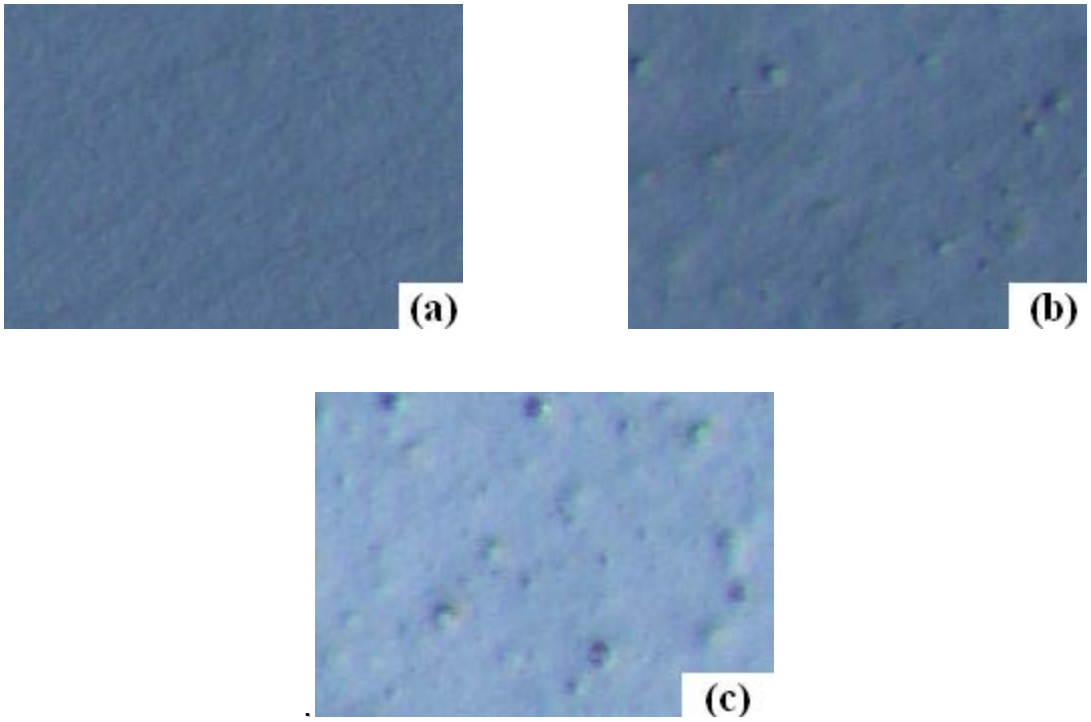


**Figure 20.** Microscopic photos of the films extruded from (a) virgin LDPE, (b) LDPE film with 2% β-CD , and (c) BHT-β-CD-IC LDPE film (magnification 80x).

As shown in Figure 20, LDPE film is very clear and does not show any granule aggregation. This leads to the conclusion that during extrusion the LDPE pellets were homogenously mixed with each other. On the other hand, in the β-CD LDPE film a very small amount of granular formation is seen more or less in the form of aggregates which are uniformly distributed in LDPE matrix. This may be due to the fact that LDPE is hydrophobic in nature and has been melted and crystallized while

β-CD is hydrophilic which results in separate phases in the blends leading to small aggregates. It has been reported that a lubricant, paraffin oil, can be used to avoid the aggregation of the β-CD in the mix of β-CD powder and the LDPE granules. However, β-CD was also found in an aggregated state although it is more or less evenly distributed within the film [57]. Hence, it may be obvious that as the amount of β-CD increases in PE matrix, the aggregates become bigger in size leading to non homogeneity. It is reported that the CD complexation results in more homogeneous distribution of the active component in the polymer matrix [58]. It is also observed from the graphs in Figure 20 that BHT-β-CD-IC LDPE film shows small aggregates uniformly distributed in the LDPE matrix over a large range similar to β-CD-LDPE film.

## 2. 3 Oxidation Induction Time/Temperature Measurements

The antioxidant BHT has been widely used for many years to stabilize polyolefins during processing, but one potential disadvantage of BHT is its relatively high volatility. It has been reported that CD inclusion complexes can provide various advantages for preventing losses due to volatilization [13, 19]. However, so far, barely any research has been conducted in measuring the oxidative performance of cyclodextrin inclusion complex with BHT in polyethylene film except for one patent [53]. Hence, there is a need to investigate the cyclodextrin inclusion complex with BHT for effectiveness as a stabilizer for polyethylene. This can provide an alternative way of replacing costlier volatile antioxidants by their CD inclusion

complexes. In this study, attempt has been made to prove that oxidative performance of BHT-β-CD-IC in LDPE film is better compared to LDPE and BHT LDPE films. The DSC scans of LDPE film, BHT LDPE film, and BHT-β-CD-IC LDPE film recorded at 190°C are shown in Figure 21. The $OIT_{time}$ values of LDPE film, BHT LDPE film, and BHT-β-CD-IC LDPE film were about 16 min, 26 min, and 35 min, respectively.

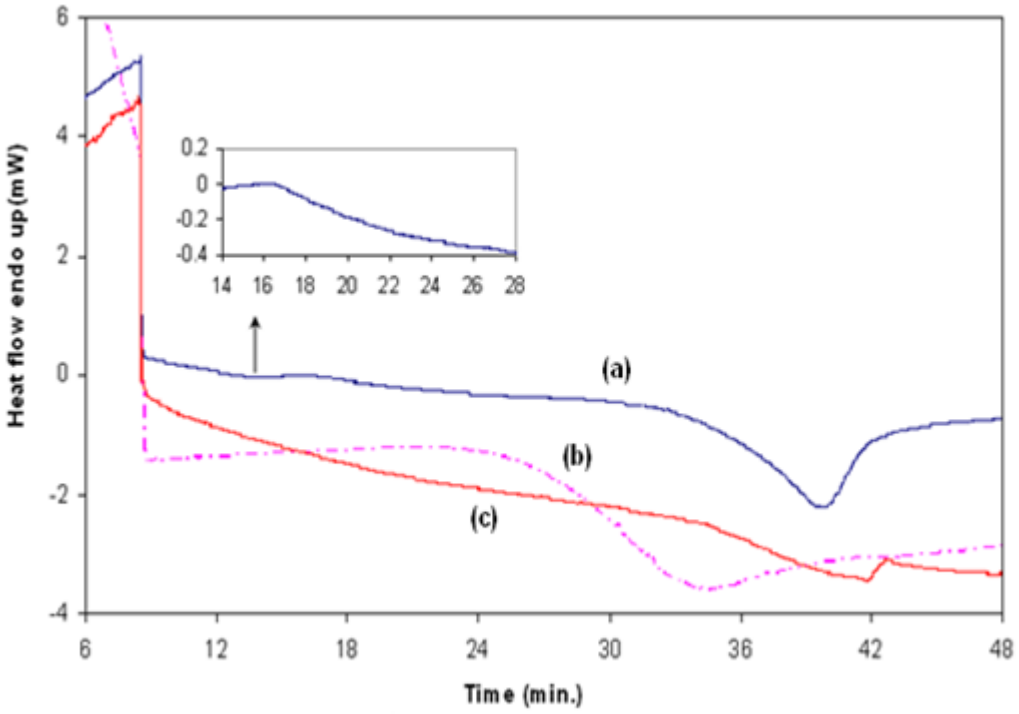


**Figure 21.** DSC scans of (a) LDPE film, (b) BHT LDPE film and (c) BHT-β-CD- IC LDPE film held at 190°C in isothermal condition

The highest induction time was observed for BHT-β-CD-IC LDPE film as compared to LDPE and BHT LDPE films. The thermal degradation of the LDPE film starts earlier than the other two films. This means that BHT-β-CD-IC LDPE film was most

resistant to oxidative degradation as compared to commercially available synthetic antioxidant BHT. Therefore, encapsulation of BHT in cyclodextrin prevents its volatilization, and it indicates that on addition of CD inclusion complex with BHT during melt processing of LDPE films can substantially increases the stability of the polymer under thermal degradation.

As shown in Figure 22, a sharp endotherm is observed for all the three films in the range of106-109ºC. This is attributed due to the melting peak of LDPE film [30]. The $T_{onset}$ values of the oxidation where the exothermic transition causes a shift in the baseline for the LDPE film, BHT-LDPE film, and BHT-β-CD-IC LDPE film are 223°C, 222°C, and 228 °C, respectively.

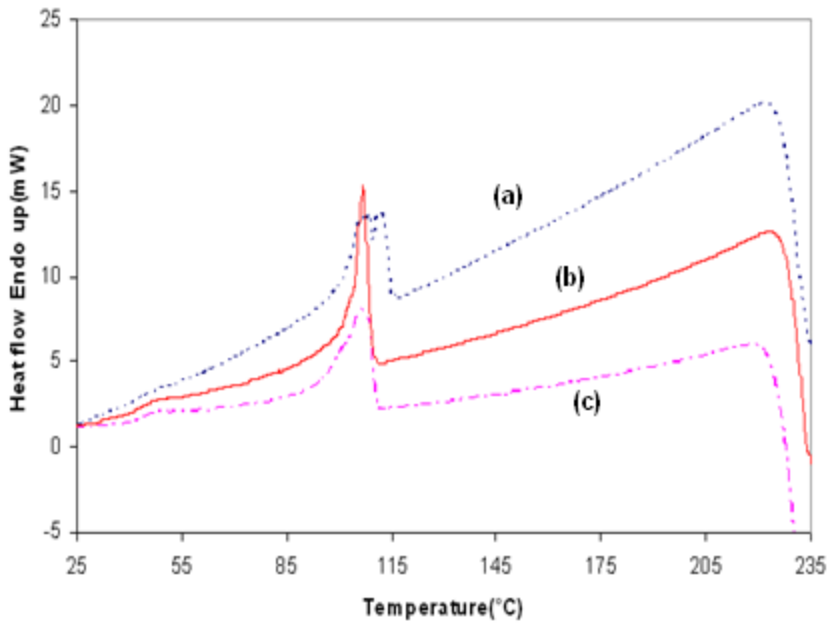


**Figure 22.** DSC scans of (a) LDPE film, (b) BHT-β-CD-IC LDPE film, and (c) BHT LDPE film and (c) under pure oxygen atmosphere at heating rate of 10ºC/min

Comparing between BHT LDPE film and LDPE film, no significant differences was observed. Hence, addition of BHT had very little effect on the LPDE film. The BHT-β-CD-IC LDPE film shows highest value of OIT temperature, although there was only a small difference as compared with BHT LDPE film and LDPE film. Therefore, our results are in agreement that the dynamic OIT method is less sensitive, as compared to the static OIT method [30].

Finally with both static and dynamic OIT measurements it was proved that BHT-β-CD- IC LDPE film offers the best resistance to oxidative degradation during processing as compared to LDPE and BHT LDPE films. It is reported that the OIT measurement gives indication of the performance of antioxidant during melt processing of polyolefins [29]. It is also reported that aging effects or presence and effectiveness of antioxidants can be analyzed with the OIT method [30]. However, OIT measurement may not be extrapolated to reflect the antioxidant performance at room temperature, because the measurement is taken at high temperatures where the polymer is in molten state. For performing measurements at lower temperatures, methods such as oven aging, oxygen uptake, etc. may be used [36].

## 2. 4 Dynamic Mechanical Thermal Analysis

Figure 23 shows that LDPE film has the lowest storage modulus value. However, addition of BHT, β-CD and BHT-β-CD-IC to virgin LDPE film increased the storage modulus in increasing order of magnitude.

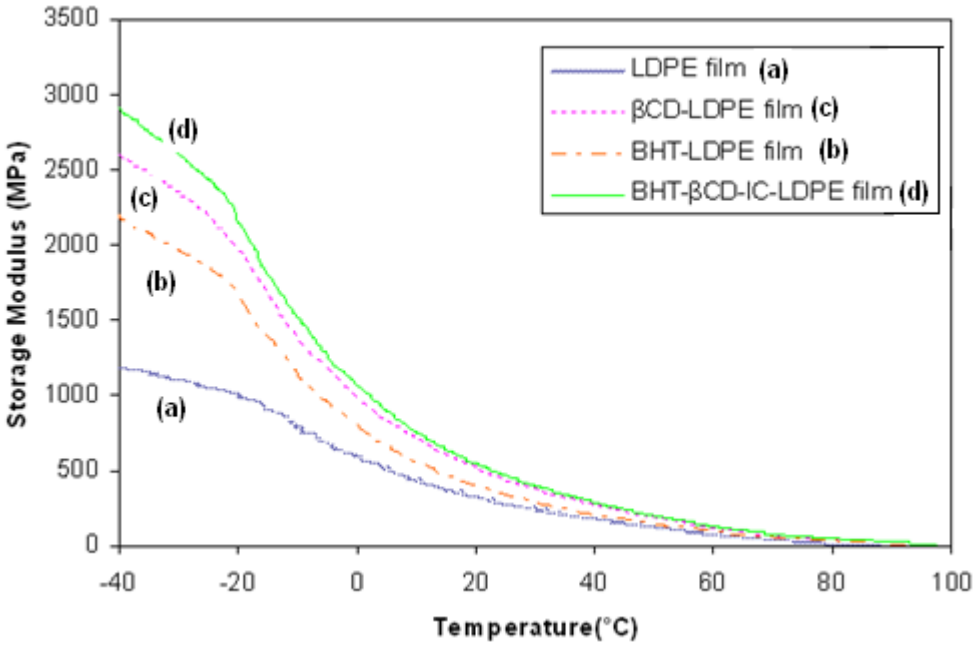


**Figure 23.** Storage modulus plot as a function of temperature

Storage modulus is related to the elastic component of the polymer. Hence, higher storage modulus values represent higher rigidity, indicating that BHT and β-CD decreases the polymer chain mobility. When comparison between BHT LDPE and β-CD LDPE was made, the LDPE film with β-CD has a higher storage modulus. This may be due to the fact that both BHT and LDPE are hydrophobic in nature which causes this blend to mix well imparting chain mobility. In the case of β-CD LDPE

film, β-CD exterior is hydrophilic in nature which causes blends to become incompatible, hence reducing its chain mobility. Therefore, β-CD LDPE has a higher elastic modulus than BHT LDPE film. In our case BHT may be acting as an anti-plasticizer, which was observed by Vidotti et al. for starch [59]. Also it can be assumed that β-CD simulates starch by acting as a filler, shown by Pedroso and Rosa [51]. In general, the storage modulus value increases due to stiffening effect of granules. Addition of β-CD to LDPE film may decrease the % elongation at break and tensile strength due to low interfacial interaction between the components of blends leading to mechanical rupture at blend interfaces [51, 60].

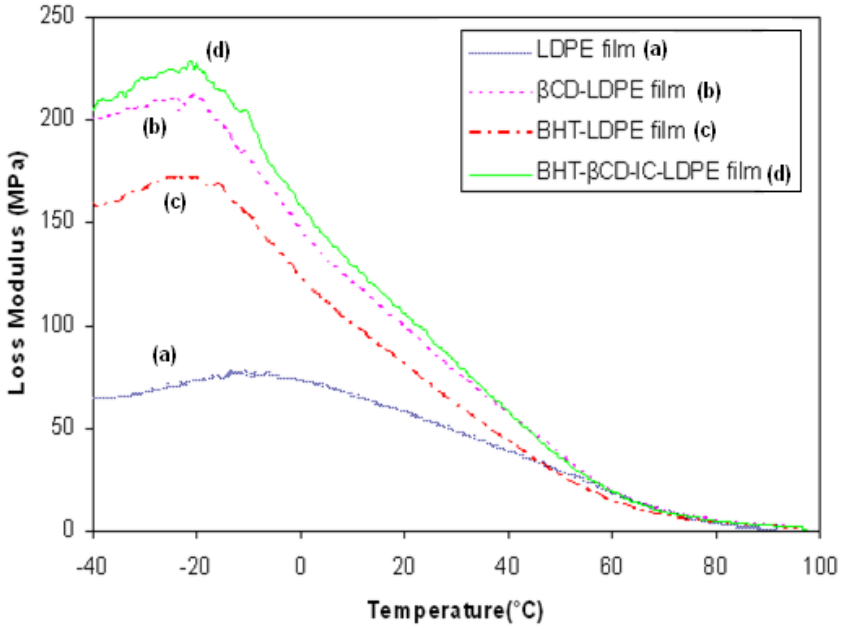


**Figure 24.** Dynamic mechanical analysis curve for loss modulus v/s temperature

Figure 24 shows loss modulus of the films versus temperature. Loss modulus ($E^{II}$) refers to loss of heat due to viscous component of the material. Lower $E^{II}$ values mean higher elastic recoveries. Hence, it can be observed that LDPE film has the lowest $E^{II}$ value followed by the addition of BHT, β-CD and BHT-β-CD-IC to LDPE films. In general, the rapid rise in the loss modulus curve shows an increase in the irreversible structural mobility of polymer causing mobility along the larger parts of individual polymer chains [40]. It is also known that the loss modulus ($E^{II}$) increases as crystallinity decreases [61]. The crystallinity of these films determined by DSC was found to be 49, 46, 40, and 37% for LDPE film, BHT LDPE film, β-CD LDPE film, and BHT-β-CD-IC LDPE films, respectively. As shown in Figure 24, LDPE film has the lowest loss modulus. However, addition of BHT, β-CD, and BHT-β-CD-IC to the LDPE film increased the loss modulus in increasing order of magnitude. The LDPE film shows a broad transition between –20 to 0ºC [41]. Also it can be observed that this transition in films decreases in temperature with the addition of BHT, βCD and BHT-β-CD-IC into the LDPE matrix. It is interesting to know that on the contrary, addition of starch to LDPE film caused increase in this relaxation temperature [51].

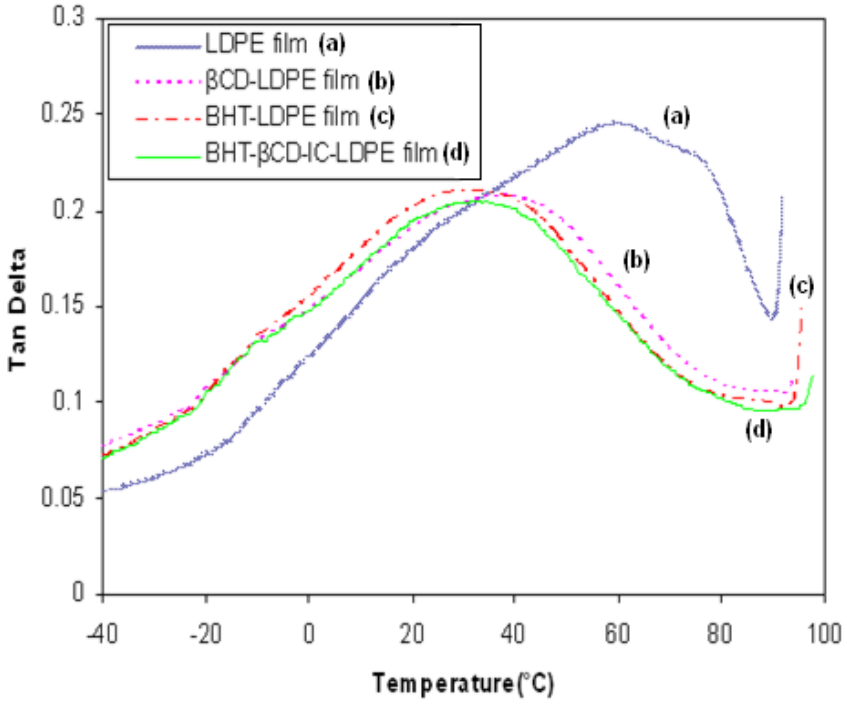


**Figure 25.** Dynamic mechanical analysis curve for tan delta v/s temperature

Tan δ is the ratio of $E^{II}/E^{I}$. Hence, lower $E^{I}$ values correspond to higher Tan δ. Tan δ can be considered as an index of viscoelasticity. Since LDPE film has lowest $E^{I}$ value, it has highest Tan $\delta$. The primary transition referred to as the glass transition ($T_g$), is generally attributed to increased mobility of main polymeric chains [39]. However, polyethylene is an unusual case. The transition in the range of –100 to –125°C is the glass transition [62]. In Figure 25, another transition of LDPE film lies in the range of 50 to 70ºC as observed by Jagannath et al. [50]. The addition of BHT, βCD and BHT-β-CD-IC causes this transition to decrease and the curves shift to lower temperatures along with the broadening of peaks over a wider temperature range.

# IV. CONCLUSIONS

The β-cyclodextrin inclusion complex with the phenolic antioxidant BHT (BHT-β-CD-IC) was successfully formed and characterized using DSC, TGA, WAXD and $^{1}$HNMR. The complex forms a cage-type crystalline inclusion compound. About 3-5wt% of BHT was contained in the large-scale inclusion complex, as determined by using UV-Vis Spectroscopy. For the first time, we extruded low density polyethylene (LDPE) films with BHT-β-CD-IC on a pilot scale. After extrusion, the amount of BHT in the films was determined using GC-MS. The results show that 44% BHT was lost from BHT-β-CD-IC LDPE films while 78% BHT was lost from the BHT LDPE film. Hence, the complex proved to be more efficient in preventing loss of BHT due to encapsulation of volatile guest. In addition, microscopy studies indicate that BHT-β-CD-IC LDPE film shows small aggregates uniformly distributed over a large range in the LDPE matrix.

The BHT antioxidant efficiency of the complex in the film was investigated using oxidation induction time/temperature (OIT) methods. The $OIT_{time}$ was 35 min for the BHT-β-CD-IC LDPE film as compared with a 26 min value for BHT LDPE films. It indicates that addition of the complex during extrusion can substantially increase the resistance towards oxidative degradation of the film. The results obtained from DMA study indicate increase in storage modulus, and loss modulus of the complex and shift in the maxima of tan δ to lower temperature in the LDPE films processed with BHT, β-CD and BHT-β-CD-IC.

# V. REFERENCES


1. Villiers, A.; Compt. Rend.; **1981**; 112; 536.
2. French, D.; Adv. Carbohydrate Chem., **1957**; 12; 189.
3. Atwood, J.L.; Davies J.E; Macnicol, D.D; Vogtle, F.; Lehn, J.M; Comprehensive Supramolecular Chemistry; Vol. 3; **1996**; Pergamon.
4. Szejtli, J.; Chem. Review; **1998**; 98; 1743-1753.
5. Valle, M.; Process Biochemistry; **2004**; 39; 1033-1046.
6. Saenger, W.; Jacob, J.; Gessler, K.; Steiner, T.; Hoffman, D.; Sanbe, H.; Koizumi, K.; Smith, S.M.; Takaha, T.; Chem. Review; **1998**; 98; 1787-1802.
7. Szejtli, J.; Encyclopedia of Nanoscience and Nanotechnology; **2004**; 2; 283-304.
8. Uekama, K.; Hirayama, F.; Arima, H.; J. of Incl. Phen. & Macro. Chem.; **2006**; 56; 3-8.
9. Uekama, K.; Hirayama, F.; Irie, T.; Chem. Review; **1998**; 98; 2045-2076.
10. Schlenk, W. Jr. Fortschr Chem. Forsch.; **1951**; 2; 92.
11. Szejtli, J.; Cyclodextrin Technology; c**1988**; Kluwer Academic Publisher.
12. Liu, L.; Guo, Q.X.; J. of Incl. Phenomena and Macrocyclic Chem.; **2002**; 42; 1-14.
13. Hedges, A.R.; Chem. Review; **1998**; 98; 2035-2044.
14. Masson, M.; Sigurdardottir, B.V.; Matthiasson, K.; Loftsson, T.; Chem. Pharm. Bull.; **2005**; 53; 958.

15. Reineccius, T.A.; Reineccius, G.A.; Peppard, T.L.; J. Agric. Food Chem.; **2005**; 53; 388.
16. Mattos, D.M.; Oliveria, L.F.C.; Nascimento, A.A.M.; Demicheli, C.P.; Sinisterra, R.D.; Appl. Organomet. Chem.; **2007**; 14; 507.
17. Verstichel, S.; Dewilde, B.; Fenyvesi, E.; Szejtli, J.; J. of Polym. Environ.; **2004**; 12; 47.
18. Whang, H.S.; Hunt, M. A.; Wrench, N.; Hockney, J.E.; Farin, C.E.; Tonelli, A.; J. of Appl. Poly. Sci.; **2007**; 106(6); 4104-4109.
19. Whang, H.S.; Tonelli, A.; J. of Incl. Phenom. & Macrocycl. Chem.; accepted in **2008**.
20. Bovey, F.A.; Winslow, F.H.; Macromolecules: an introduction to polymer science; Bell Lab.; NJ, **1979**.
21. Shlyapnikov, Y.A.; Kiryushkin, S.G.; Mar'in, A.P.; Antioxidative Stabilization of Polymers; **c1996**; Taylor & Francis.
22. Murphy, J.; Additives for Plastics Handbook; II ed.; **2001**; Kindlington; Oxford; U.K.
23. http://www.specialchem4adhesives.com/tc/antioxidants/
24. Lee, R.E.; Narayan, S.; Pallini, L.; Zenner, J.M.; Annual Tech. Conf.- Society of Plastics Engineers; **1999**; 57$^{th}$(Vol. 2); 2308-2311.
25. Corrales, T.; Abrusci, C.; Allen; N.S.; Peinado, C.; Catalina, F.; Recent Research Developments in Photochem. & Photobio.; **2004**; 7; 101-138.

26. Pethrick, R.A.; Polymer Yearbook; **c1984-2003**; Harwood Academic Publisher; 133-153.
27. Knobloch, G.; Kanouni, M.; Fagouri, C.; 168th Tech. Meeting of Rubber Division; ACS; Nov. **2005**; 1-5.
28. Knobloch, G.; Kanouni, M.; Fagouri, C.; Ciba Specialty Chemicals; Rubber World; Aug. **2006**; 22-27.
29. ASTM D 3895-07, Standard Test Method.
30. Characterization of PE with DSC and DMA; Netzsch Applcations Laboratory Newsletter; 09-**2005**-03; 1-11.
31. Schmid, M.; Ritter, A.; Affolter, S.; J. of Thermal Analysis & Calorimetry; **2006**; 83; 367-371.
32. Schmid, M.; Affolter, S.; Polymer Testing; **2003**; 22; 419-428.
33. Kovarova, J.; Rotschova, J.; Brede, O.; Burgers, M.; Canadian J. Chem.; **1995**; 73; 1862-1868.
34. Padron, A.J.C.; Suarez, F.P.; Berroteran, H.; Polym. Degradation & Stability; **1986**; 14; 295-306.
35. Bharel, R.; Anand, R.C.; Choudhary, V.; Varma, I.K.; Poly. Degaradtion & Stability; **1992**; 38; 107-112.
36. Breese, K.D.; Lamethe, J.F.; DeArmitt, C.; Poly. Degrad. & Stability; **2000**; 70; 89-96.
37. Neilsen, L.E.; Mechanical Properties of Polymers and Composites; **c1994**; Vol. 1; Dekker, M.; Newyork.

38. Jones, D.S.; Intl. J. of Pharmaceutics; **1999**; 179; 167-178.
39. Hunt, B.J.; James, M.I.; Polymer Characterisation; **c1993**; Blackie Academic & Professional; N.Y.; pg. 195.
40. Sepe, M.P.; Dynamic Mechanical Analysis for Plastics Engg.; **c1998**; Norwich, N.Y.
41. Popli, R.; Glotin, M.; Mandelkern, L.; J. of Poly. Sc.: Poly. Physics Ed.; **1984**; 22; 407-448.
42. Takayanagi, M.; Matsuo, T.; J. Macromol. Sci. Phys.; B1; **1967**; 407.
43. Bohn, V.L.; Kolloid, Z.; **1964**; 10; 194.
44. Eby, R.K.; Colson, J.P.; J. Accoust. Soc. Am.; **1966**; 39; 506.
45. Illers, V.K.H.; Kolloid Z. Z. Polym.; **1973**; 251; 394.
46. Moore, R.S.; Matsuoka, S.; J. Polym. Sc. Part C; **1963**; 5; 163.
47. Schmieder, V.K.; Wolf, K.; Kolloid Z.Z. Polym.; **1953**; 134; 149.
48. Nielsen, L.E.; J. Polym. Sci.; **1960**; 42; 357.
49. Mori, T.; Dong, T.; Yazawa; K.; Inoue, Y.; Macromol. Rapid. Commun.; **2007**; 28; 2095-2099.
50. Jagannath, J.H.; Nadanasabapathi, S.; Bawa, A.S.; J. of Applied Polym. Sci.; **2006**; 99; 3355-3364.
51. Pedroso, A.G.; Rosa, D.S.; Carbohydrate Polymers; **2005**; 59; 1-9.
52. Vora, J.; Boroujerdi, M.; Drug Development & Industrial Pharmacy; **1995**; 21(4); 495-502.

53. Bernard, D.; Gilles, M.; Etienne, W.; Inclusion comp. of phenolic antioxidants in cyclodextrins for use in poly.; Rhone-Poulec Chimie SA, Fr.; Fr. Demande; **1992**; FR patent 2665169.
54. Linder, K.; Saenger, W.; Carbohydrate Research; **1982**; 99; 103.
55. Trotta, F.; Zanetti, M.; Camino, G.; Polym. Degradation and Stability; **2000**; 69; 373-379.
56. Bender, M.L.; komiyama, M.; Cyclodextrin Chemistry; Spring- Verlag Berlin Heidelberg; N.Y.; **1978**.
57. Fenyvesi, E.; Balogh, K.; Siro, I.; orgovanyi; J.; Senyi, J.M.; Otta, K.; Szente, L.; J. Incl. Phenom. Macrocycl. Chem.; **2007**; 57; 371-374.
58. Szejtli, J.; Fenyvesi, E.; Cyclodextrins in active and smart packaging; Cyclodextrin News; **2005**; 19; 213-216; 241-245.
59. Vidotti, S.E; Chinelatto; A.C.; Hu, G.H.; Pessan, L.A.; J. of Appl. Polym. Sci.; **2006**; 101; 825-832.
60. Garg, S.; Jana, A.K.; Indian Chem. Engr. Sec. A; **2006**; 48; 185-189.
61. Murayama,T; Dynamic Mechanical Analysis of Polymeric Materials; Elsivier Scientific Publishing Company;**1978**.
62. Matsuko, S.; Relaxation Phenomena in Polymers; Hanser Publishers; **1992**.